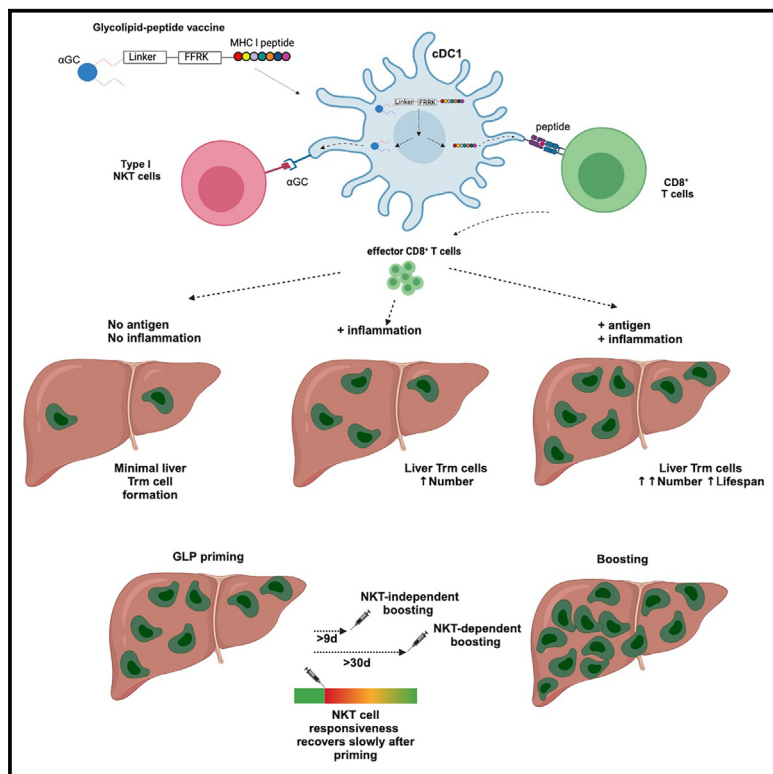


Mechanistic insight into the induction of liver tissue-resident memory CD8⁺ T cells by glycolipid-peptide vaccination

Graphical abstract



Authors

Yu Cheng Chua, Sarah L. Draper,
Shirley Le, ..., William R. Heath,
Gavin F. Painter, Lauren E. Holz

Correspondence

lauren.holz@unimelb.edu.au

In brief

Liver tissue-resident memory T (Trm) cells are important for liver-stage malaria immunity. Chua et al. demonstrate that optimal generation of long-lived liver Trm cells requires priming by cDC1, post-priming exposure to antigen and inflammation, and consideration of the timing and types of vaccine boosters. These findings inform future vaccine design.

Highlights

- T cell priming by cDC1 is important for generation of liver Trm cells
- Post-priming antigen and inflammation exposure enhances liver Trm cell longevity
- Quicker boosting of liver Trm cell numbers using NKT cell-independent vaccine
- Antigen persists for at least 56 days after GLP vaccination



Article

Mechanistic insight into the induction of liver tissue-resident memory CD8⁺ T cells by glycolipid-peptide vaccination

Yu Cheng Chua,^{1,9} Sarah L. Draper,^{2,9} Shirley Le,¹ Maria N. de Menezes,¹ Mitch Ganley,¹ Zhengyu Ge,¹ Ariane Lee,¹ Taylah Phabmixay,¹ Daria Hirschmann,¹ Sage A. Robinson,³ Peck Szee Tan,⁴ Kirsteen M. Tullett,⁴ Regan J. Anderson,² Dhilshan Jayasinghe,⁵ Anton Cozijnsen,⁶ Mireille H. Lahoud,⁴ Irina Caminschi,^{1,4} Lynette Beattie,¹ Geoffrey I. McFadden,⁶ David S. Larsen,³ Tsuneyasu Kaisho,⁷ Stephanie Gras,^{4,5} Ian F. Hermans,⁸ Benjamin J. Compton,² William R. Heath,^{1,10} Gavin F. Painter,^{2,10} and Lauren E. Holz^{1,10,11,*}

¹Department of Microbiology and Immunology, The Doherty Institute for Infection and Immunity, The University of Melbourne, Melbourne, VIC 3000, Australia

²Ferrier Research Institute, Victoria University of Wellington, Lower Hutt 5010, New Zealand

³Department of Chemistry, University of Otago, Dunedin 9016, New Zealand

⁴Immunity Program, Monash Biomedicine Discovery Institute and Department of Biochemistry and Molecular Biology, Monash University, Clayton, VIC 3168, Australia

⁵Department of Biochemistry and Chemistry, La Trobe Institute for Molecular Science, La Trobe University, Bundoora, VIC 3083, Australia

⁶School of BioSciences, The University of Melbourne, Parkville, VIC 3052, Australia

⁷Department of Immunology, Institute of Advanced Medicine, Wakayama Medical University, Wakayama 641-8509, Japan

⁸Malaghan Institute of Medical Research, Wellington 6012, New Zealand

⁹These authors contributed equally

¹⁰These authors contributed equally

¹¹Lead contact

*Correspondence: lauren.holz@unimelb.edu.au

<https://doi.org/10.1016/j.celrep.2025.115295>

SUMMARY

We recently demonstrated that vaccines comprising antigenic peptides conjugated to a glycolipid agonist, termed glycolipid-peptide (GLP) vaccines, efficiently generate substantial numbers of long-lived CD8⁺ liver-resident memory T (Trm) cells that are crucial for protection against malaria liver-stage infection. To understand the underlying mechanism, we examined the prerequisites for priming, differentiation, and secondary boosting of liver Trm cells using these GLP vaccines. Our study revealed that generation of long-lived liver Trm cells relies on CD8⁺ T cell priming by type 1 conventional dendritic (cDC1) cells, followed by post-priming exposure to a combination of vaccine-derived inflammatory and antigenic signals. Boosting of liver Trm cells is feasible using the same GLP vaccine, but a substantial delay is required for optimal responses due to natural killer T (NKT) cell anergy. Overall, our study unveils key requirements for the development of long-lived liver Trm cells, offering valuable insights for future vaccine design.

INTRODUCTION

Malaria remains a global health crisis. In 2022, 84 countries were still endemic for malaria, with more than 240 million cases and over 600,000 deaths.¹ This devastating disease is caused by *Plasmodium* species parasites that infect humans through *Anopheles* mosquitoes. *Plasmodium falciparum* is the largest killer, accounting for >90% of deaths globally.¹ Within hours of being bitten by a *Plasmodium*-carrying mosquito, parasites referred to as sporozoites migrate to the liver where they infect hepatocytes and begin a replication/maturation cycle lasting approximately 2 days in mice and a week in humans. At the completion of the liver stage, thousands of merozoites exit the liver and begin invading red blood cells. At this stage, the infected human host begins to develop malaria symptoms.

Some merozoites develop into female and male gametocytes. If consumed by a mosquito during a blood meal, these gametocytes can undergo a sequence of events leading to the accumulation of infectious sporozoites in the insect salivary glands and completion of the parasite life cycle in the mosquito host.²

Generating immunity against the clinically silent pre-erythrocytic stages (i.e., sporozoite and liver-stages) is necessary to prevent malaria disease. Current approved vaccines RTS,S and R21 rely on the generation of neutralizing antibodies to target migrating sporozoites before they reach the liver. While R21 has shown the most promise in clinical trials,³ it would greatly benefit if combined with vaccines targeting other stages of the life cycle, including the liver and blood stages. Durable immunity against malaria liver-stage infection requires large numbers of memory CD8⁺ T cells that are poised to rapidly kill



Plasmodium-infected hepatocytes upon antigen encounter.^{4–6} Benefiting from its localization in the liver, this response is primarily mediated by liver-resident memory T (Trm) cells,^{7,8} although effector memory T (Tem) cells that subsequently migrate to this tissue can also potentially contribute.⁹ Consequently, vaccines that primarily generate liver Trm cells can be highly effective at controlling liver-stage malaria infection.^{7,8,10–12} This includes vaccination with radiation-attenuated sporozoites (RAS), which induces protection that is highly dependent on liver Trm cells.⁷ Intravenous (i.v.) vaccination is the most effective route for RAS to generate liver Trm cells,^{13,14} with their precursors initially primed by type 1 conventional dendritic (cDC1) cells in the spleen¹⁵ and later converted to Trm cells in the liver after local exposure to the RAS-associated antigenic and inflammatory signals.¹⁶ Such whole-sporozoite vaccines have already progressed through several clinical trials, with some promising efficacy observed in malaria-naïve individuals,^{13,14,17,18} although less favorable findings have been associated with malaria-endemic regions.^{19,20} Protection, when achieved, generally relies on administration of very high numbers of sporozoites and multiple immunizations, further limiting utility in the field.

More recently, we described a simple anti-malarial glycolipid-peptide (GLP) vaccine that consists of a CD8⁺ T cell epitope conjugated to a modified form of the α -galactosylceramide (α -GalCer) glycolipid, a potent agonist of type I natural killer T (NKT) cells.¹² This vaccine is superior to RAS in several aspects, including its ability to generate substantially more antigen-specific liver Trm cells after a single immunization.¹² These Trm cells also exhibit a much longer lifespan (i.e., half-life of >200 days versus about 30 days for RAS immunization), facilitating long-term sterile immunity against malaria infection.¹² However, little is known about the mechanistic basis that underpins the remarkable capacity of this GLP vaccine to generate long-lived liver Trm cells.

Our current model hypothesizes that, during the primary immune response, the GLP vaccine is acquired by antigen-presenting cells (APCs), which process and present vaccine-derived components (α -GalCer and peptide) to activate both type I NKT cells and CD8⁺ T cells.^{12,21,22} The nature of the APC, however, remains somewhat uncertain. In response to GLP-derived α -GalCer presented by APCs, NKT cells become activated and can provide help to CD8⁺ T cells by “licensing” APCs through CD40–CD40L signaling and inflammatory cytokines.¹² Furthermore, while the GLP vaccine can activate CD8⁺ T cells in the spleen, it is also likely to provide inflammatory and antigenic signals in the liver, the former via NKT cell activation in this tissue. Exposure to inflammatory stimuli is known to aid liver Trm cell formation,¹⁶ as does local antigen encounter,^{7,10,11} but it remains unclear whether these signals provided by GLP vaccination contribute to vaccine efficacy.

In our previous study, we demonstrated the feasibility of expanding the liver Trm cell numbers by a 30-day homologous prime-boost immunization with GLP vaccines.¹² NKT cell anergy is a common phenomenon that occurs after α -GalCer-mediated stimulation^{23,24} but agonist-antigen conjugation reduces NKT cell hypo-responsiveness,²¹ suggesting that such an undesirable effect of NKT cells may be less of a concern for GLP vac-

cines. However, optimization of the prime-boost immunization schedule and exploration of whether a heterologous booster immunization can be used as an alternative to a homologous booster remains unanswered.

In this study, we characterize the priming, differentiation, and secondary boosting of liver Trm cells, providing insight into the developmental requirements for liver Trm cells, which can be exploited for designing next-generation vaccines aimed to target liver Trm cells for immunity against hepatotropic pathogens.

RESULTS

Liver Trm cells induced by GLP vaccines are long lived

In our previous study,¹² we demonstrated that a GLP vaccine (RPL6 GLP; Figure S1) containing the NVFDFNNL (NVF) epitope of the *Plasmodium berghei* ANKA (PbA) ribosomal protein L6 (RPL6) can generate long-lived liver Trm cells in C57BL/6 (B6) mice, with minimal decay after 200 days post vaccination. Given that this assessment was somewhat limited in duration, we sought to extend analysis to over 300 days. By pooling data from the previous and current studies using the RPL6 GLP vaccine, we found that the number of RPL6-specific liver Trm cells remained relatively stable up to 309 days post immunization (Figures 1A and S2), revealing a population half-life of 236 days (95% confidence interval, 170–390 days; $R^2 = 0.1387$) (Figure 1B). To test the durability of protection against sporozoite challenge, additional RPL6 GLP-vaccinated mice from the indicated time points were challenged with 200 PbA sporozoites and then assessed for parasitemia up to day 12. Lack of parasitemia at this point indicates protection from infection. This showed that a large proportion of mice were protected against sporozoite challenge as late as 309 days post vaccination, and, while appearing to wane with time, it was not significantly different from the 90%–100% protection observed up to day 200 (Figure 1C).

To determine whether the long-lived nature of the response to the RPL6 GLP vaccine extended to other antigens, we examined immunity to ovalbumin (OVA). Groups of B6 mice were vaccinated i.v. with GLP vaccines containing either an RPL6 or OVA epitope (Figure S1) and were then assessed for memory T cell responses in the liver on days 45, 145, and 210 (Figure 1D). Both vaccines generated very stable liver Trm cell populations that persisted for at least 210 days (Figure 1D). Together, these data suggest that the GLP vaccines induce long-lived liver Trm cells that are highly protective against sporozoite challenge.

A rapid and robust primary CD8⁺ T cell response to the GLP vaccine

To protect against liver infection, it would be ideal to induce the largest Trm cell responses possible, perhaps by boosting primary responses. Before extensively analyzing boosting, however, we considered it important to better understand where the responses to GLP vaccination were initiated and by which APCs. To determine the site of priming, B6 mice were adoptively transferred with naive cell trace violet (CTV)-labeled OVA-specific transgenic CD8⁺ T (OT-I) cells and, 1 day later, vaccinated i.v. with an OVA or RPL6 GLP vaccine. We used the OVA model system here as a readout rather than the PbA.RPL6 malaria

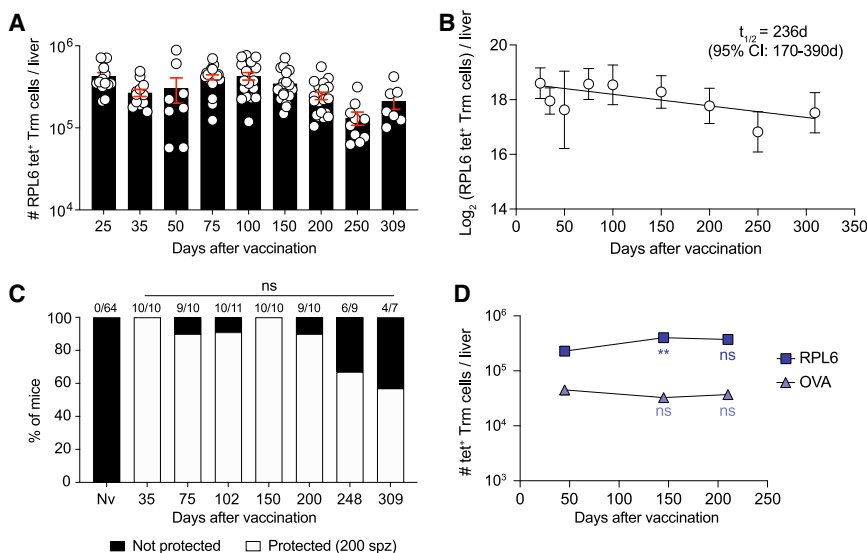


Figure 1. Long-lived liver Trm cells protect against malaria

B6 mice were i.v. immunized with RPL6 GLP and then assessed for RPL6-specific memory CD8⁺ T cells at the indicated time points post vaccination by flow cytometry.

(A) Enumeration of RPL6-tetramer (tet)⁺ liver Trm cells at different time points after vaccination. Gating shown in Figure S2. Mean ± SEM.

(B) Linear regression analysis of the half-life of RPL6-specific liver Trm cells, with the estimated half-life ($t_{1/2}$) shown. Mean ± SD. Data for each indicated time point are pooled from two to four independent experiments ($n = 7$ –20 mice per group).

(C) The remaining vaccinated mice at each indicated time point, and naive (Nv) B6 mice, were i.v. challenged with 200 PbA sporozoites, and blood parasitemia was measured up to day 12 post infection. Shown is the percentage of protected (white bars) and unprotected (black bars) mice after sporozoite challenge. Numbers above bars indicate the number of mice that were protected

against the 200 sporozoite challenge over the total number of mice challenged. Data for each individual time point are pooled from two or more independent experiments ($n = 7$ –64 mice per group) and protection compared using a two-sided Fisher's exact test.

(D) B6 mice were i.v. immunized with RPL6 GLP or OVA GLP vaccine and then assessed for tet⁺-specific memory CD8⁺ T cells at the indicated time points post vaccination by flow cytometry. Mean ± SEM is shown. Data were log transformed and compared using the one-way ANOVA with Dunnett's multiple comparison test with cell counts at day 45.

ns, not significant; ** $p < 0.01$.

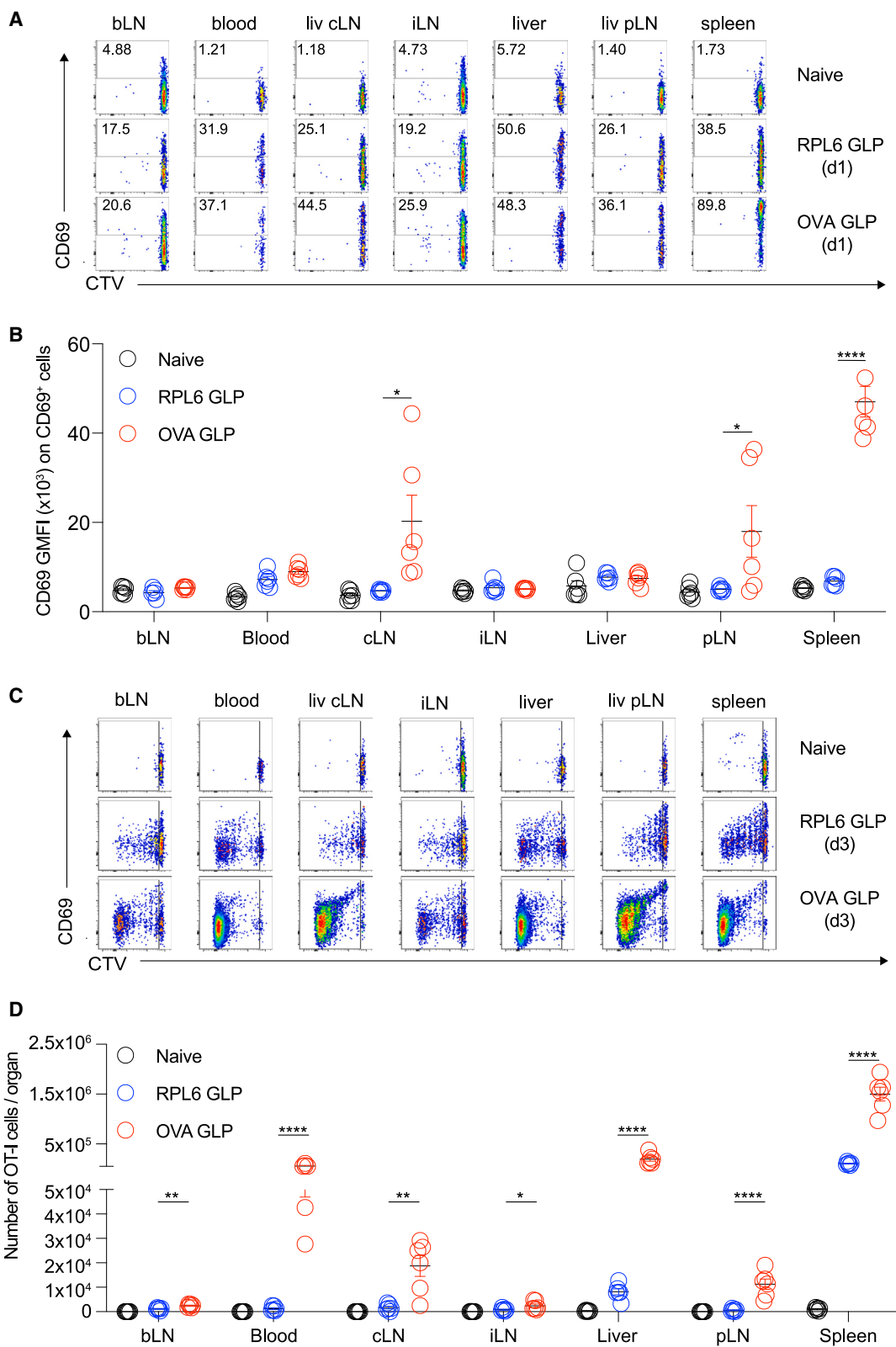
model because transgenic naive PbT-I cells,¹⁵ which recognize RPL6,²⁵ show low-level homeostatic proliferation *in vivo* in the absence of antigen, which impairs clear interpretation of T cell activation in this model. Such homeostatic proliferation is not evident in the OT-I system. After vaccination with the OVA or RPL6 GLP, the kinetics of OT-I cell activation and proliferation was examined in various tissues (spleen, several lymph nodes, liver, and blood) from days 1 to 3 by examining upregulation of the activation marker CD69 and dilution of the CTV dye. This revealed the rapid upregulation of CD69 in all tissues after vaccination with either GLP vaccine (Figure 2A), but the extent of CD69 upregulation was significantly higher in the spleen and liver draining lymph nodes (celiac and portal lymph nodes) of mice vaccinated with a GLP-expressing cognate antigen (Figure 2B). Similarly, proliferation of transferred OT-I cells was evident in mice vaccinated with either GLP vaccine, although the rate of proliferation was much higher for cognate antigen (Figure 2C). Furthermore, accumulation of cells only occurred after priming with cognate antigen (Figure 2D). These data suggest that responses are initiated predominantly in the spleen and, to a lesser extent, the liver-draining lymph nodes of mice vaccinated with GLPs. Proliferation of cells can be triggered by exposure to inflammatory signals alone, but this is insufficient to promote extensive cell division and accumulation of responding cells, which requires cognate antigen.

cDC1 cells are required for CD8⁺ T cell responses to GLP vaccines

While T cell activation by GLP vaccines appeared widespread, we expected responses to be dependent upon dendritic cells (DCs) as our previous studies showed that effector CD8⁺ T cell responses to GLP vaccines were impaired in mice lacking

Batf3,²² a transcription factor essential for the development of cDC1.²⁶ One caveat with this finding, however, was that CD8⁺ T cells can express *Batf3*, which may have influenced responses.²⁷ To circumvent this issue and to further examine the role of cDC1 in priming, we took advantage of XCR1-DTR mice in which cDC1 can be conditionally depleted by treatment with diphtheria toxin (DT).²⁸

To assess the role of cDC1 in GLP vaccination, XCR1-DTR mice were either left untreated or were injected with DT to deplete cDC1 before both groups were vaccinated with the RPL6 GLP vaccine and then >21 days later assessed for endogenous RPL6-specific memory CD8⁺ T cell responses. Splenic CD8⁺ Trm cells were defined as CD69⁺ CD62L[−] KLRG1[−] CXCR6⁺ (Figure S2E) based on previous observations using parabiotic mice.^{29,30} As a control, groups of non-transgenic B6 mice were subjected to similar treatment. This analysis revealed extensive depletion of cDC1 but not cDC2 in XCR1-DTR mice treated with DT, no effect in B6 controls (Figures 3A–3C), and subsequent impairment of induction of memory CD8⁺ T cell responses in the spleen (Figure 3D) and liver (Figures 3E and 3F). This included a significant loss of the capacity to generate liver Trm cells (Figures 3E and 3F). Early analysis of RPL6-specific T cell responses in the livers of mice depleted of cDC1 prior to vaccination revealed this defect was apparent within 5 days of vaccination (Figures S3A–S3C), suggesting the diminished memory response was a result of impaired priming rather than an effect on Trm differentiation in the liver. Similarly, depletion of cDC1 at day 7 after vaccination showed no significant impact on memory T cell formation (Figures S3D and S3E), indicating that cDC1 were likely the cells priming CD8⁺ T cells and not acting as drivers of secondary T cell expansion as seen in other settings.^{31,32} Cytokine blockade early after GLP vaccination



(legend on next page)

revealed interleukin (IL)-12p40 and interferon (IFN)- γ were not essential for liver Trm cell formation (Figure S3F).

Of note, in the absence of cDC1, NKT cell activation, as measured by increased numbers of NKT cells in the spleen and liver, or by downregulation of CD69 or NK1.1 on these cells, was only modestly affected (Figures 3G–3L and S3G), suggesting a redundant role for this DC subset in NKT cell activation. Together, these data indicate an essential role for cDC1 in generating robust CD8 $^{+}$ T cell memory responses upon GLP vaccination but suggest NKT cells can be activated by additional cell types.

GLP-derived antigen and associated inflammation promotes seeding and persistence of liver Trm cells

While these studies indicated CD8 $^{+}$ T cell activation required cDC1 for induction of optimal memory, it was unclear whether GLP vaccination simply initiated robust T cell activation that led directly to liver Trm cell formation or whether post-activation signals were needed to facilitate this process. Previous studies showed that *in vitro*-activated T cells can intrinsically differentiate into liver Trm cells when transferred *in vivo* but that further exposure to inflammation or antigen, particularly in the liver, enhances Trm cell generation.¹⁶ To assess whether post-activation events provided by GLP vaccination (e.g., liver inflammation or antigen presentation) can enhance liver Trm cell formation, we activated OT-I cells *in vitro* using peptide and then 4 days later adoptively transferred these cells into B6 mice that were left untreated, treated with α -GalCer, or injected with a GLP vaccine containing the specific antigen (OVA) or an irrelevant control antigen (RPL6). This latter group, and the α -GalCer group, served to provide an inflammatory stimulus without an antigenic stimulus. After 30 days, flow cytometry analysis showed that transfer of activated OT-I cells into mice immunized with either of the GLP vaccines, or with α -GalCer, significantly increased the generation of memory T cells in the liver, with the highest number of liver Trm cells induced by the GLP vaccine containing the cognate antigen (i.e., OVA) (Figures 4A–4C). In settings where irrelevant antigen was used, liver Trm cell formation was aided by IFN- γ and was not dependent on cDC1 (Figure S4A). Significantly ($p < 0.01$) more memory OT-I cells were also generated in the spleens of mice immunized with either of the GLP vaccines (Figure 4D).

These data indicate that the combination of antigen and inflammation provided by a GLP vaccine can enhance liver Trm cell formation post T cell activation but did not assess the role of antigen exposure alone. To address this point, we also compared responses when *in vitro*-activated OT-I cells were

transferred into B6 mice vaccinated with β -ManCer-OVA (β MC-OVA), an OVA GLP vaccine containing a rearranged version of β -mannosylceramide^{33,34} that is expected to release a weak NKT cell agonist upon intracellular processing (Figure S1). This vaccine induced a very small increase in liver Trm cells (Figures 4E and 4F) and, as expected, no change in NKT cell activity (Figures S4B–S4D) or the number of circulating memory T cells (Tem and central memory [Tcm] cells) (Figure 4G), suggesting antigen exposure on its own (without inflammation) had limited influence on liver Trm formation.

Our previous work showed liver Trm cells differentiated from adoptively transferred *in vitro*-activated effector T cells have a relatively short half-life of 30 days.¹⁶ Given the ability of GLP vaccines to generate long-lived Trm cells (Figure 1B),¹² we wondered whether this related to initial priming or to some aspects post initial activation (e.g., inflammation and/or antigen presentation in the liver). To test whether exposure to the components of the GLP vaccine post T cell activation could alter the lifespan of liver Trm cells, we generated *in vitro*-activated OT-I cells and then exposed these cells to antigenic and/or inflammatory signals generated by the GLP vaccines *in vivo*. Using the same experimental setup as described above, longitudinal analysis of memory OT-I cells in the liver at various time points after GLP vaccination revealed a general decline in the number of Trm cells over time, with varying half-lives between groups. While exposure of activated OT-I cells to RPL6 GLP (i.e., inflammation alone) failed to improve the half-life of liver OT-I Trm cells ($t_{1/2} = 30$ days) compared to those formed in the unvaccinated controls ($t_{1/2} = 28$ days), those boosted with OVA GLP vaccine exhibited an increased half-life ($t_{1/2} = 58$ days) (Figure 4H). These data indicated that the longevity of liver Trm cells could be increased somewhat by post-priming exposure to a GLP-supplied antigenic signal, likely in combination with its inflammatory signal. At this stage, the contribution of priming versus post-priming effects on liver Trm cell longevity remains unclear.

Together, these data indicated that, while antigen exposure alone had minimal effect on liver Trm cell formation post activation, inflammation induced by NKT cell activation could enhance differentiation into liver Trm cells. Furthermore, the combination of antigen and inflammation enhanced liver Trm cell longevity.

GLP-derived antigen persists long term in the tissues

Given the demonstrated role for antigen and inflammation in extending half-life of Trm cells formed from *in vitro*-activated OT-I cells (Figure 4H), we wanted to determine whether the extraordinarily long half-life of Trm cells generated by GLP vaccines

Figure 2. Intravenous GLP vaccination induces CD8 $^{+}$ T cell activation in the spleen and liver-draining lymph nodes

B6 mice were adoptively transferred with 10^6 CTV-labeled OT-I cells 1 day prior to i.v. vaccination with OVA or RPL6 GLP vaccines. Various organs were harvested between days 1 and 3 post vaccination for flow cytometry analysis.

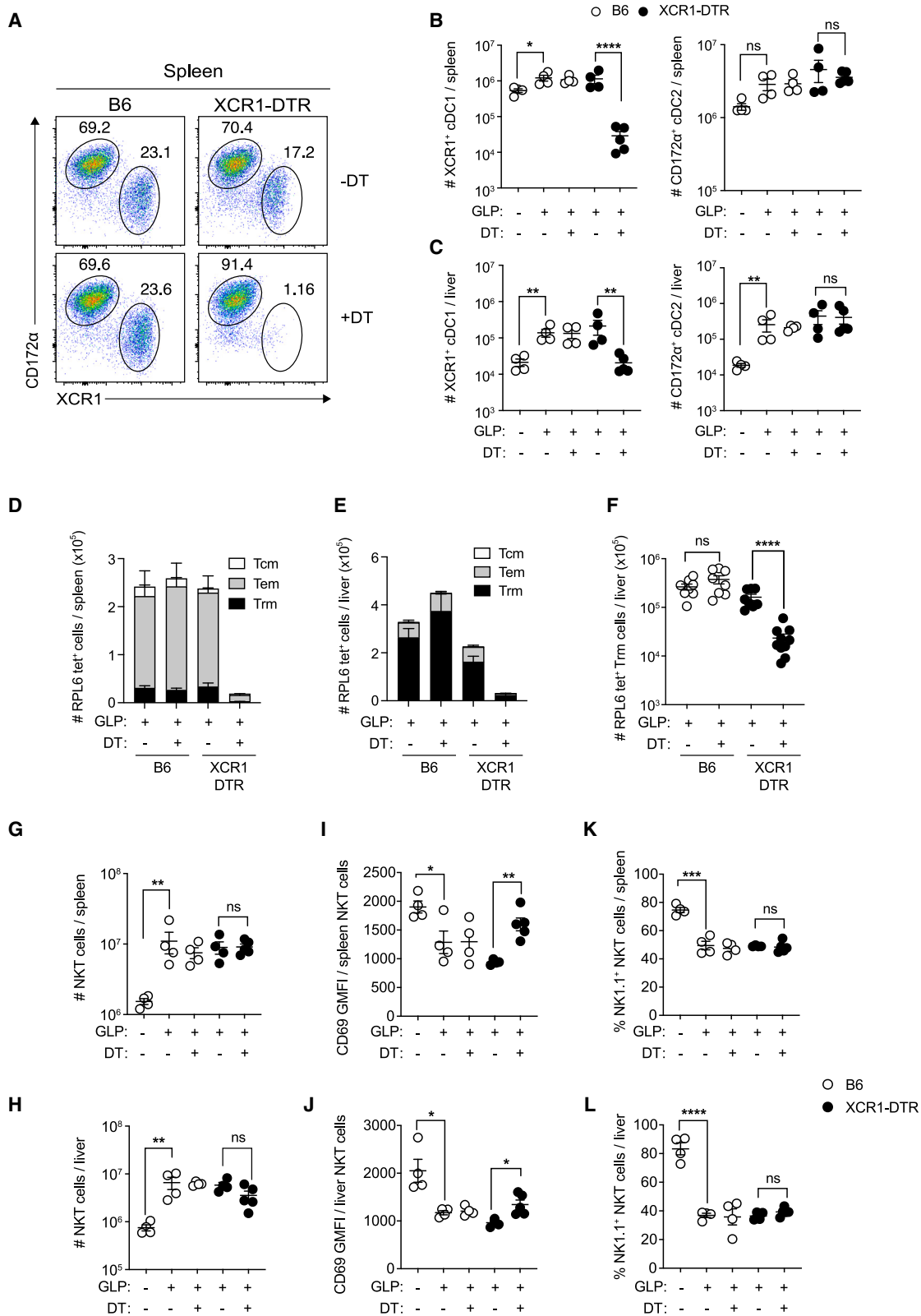
(A) Representative fluorescence-activated cell sorting (FACS) plots of CD69 expression against CTV dilution (proliferation) on OT-I cells in the indicated tissues at day 1 post vaccination. Note that all FACS plots were concatenated from three individual mice due to low OT-I cell recovery from these tissues.

(B) CD69 GMFI on CD69 $^{+}$ OT-I cells in naive (black), RPL6 (blue), and OVA GLP (red) vaccinated mice at day 1 post vaccination. Mean \pm SEM. Data are pooled from two independent experiments ($n = 6$ mice per group). Tissues in vaccinated mice were compared using an unpaired t test.

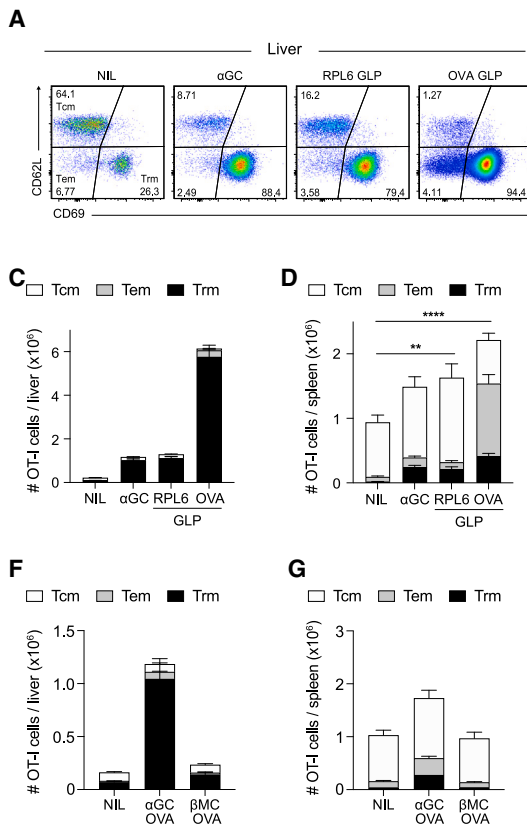
(C) Representative FACS plots of CD69 expression against CTV dilution (proliferation) on OT-I cells in the indicated tissues at day 3 post vaccination.

(D) Number of dividing OT-I cells in naive (black), RPL6 (blue), and OVA GLP (red) vaccinated mice at day 3 post vaccination. Mean \pm SEM. Data are pooled from two independent experiments ($n = 6$ mice per group).

Tissues in vaccinated mice were compared using an unpaired t test. ns, not significant; * $p < 0.05$; ** $p < 0.01$; *** $p < 0.0001$; liv, liver; liv pLN, liver portal lymph node; liv CLN, liver celiac lymph node; bLN, brachial lymph node; iLN, inguinal lymph node.



(legend on next page)



indicated time points post vaccination, with estimated half-life of liver Trm cells ($t_{1/2}$) indicated for each group ($n = 10-15$ mice per group).

Data in (B), (D), and (E) were log transformed and then compared by the one-way ANOVA with Tukey's multiple comparison test. Data in (F) were log₂-transformed and the slopes were compared using a simple linear regression. * $p < 0.05$, ** $p < 0.01$, *** $p < 0.0001$.

correlated with antigen persistence. To test this idea, groups of B6 mice were immunized with an OVA GLP or an irrelevant RPL6 GLP vaccine, and at various time points later were adoptively transferred with naive CTV-labeled OT-I cells. Proliferation of OT-I cells in the spleen and liver was then assessed 2 days post transfer. This revealed antigen-specific OT-I proliferation, albeit at very low levels, in the liver as late as 42 days post vaccination (Figures 5A and 5B), indicating long-term antigen persistence. A similar phenomenon was observed in the spleen up to

28 days after vaccination with OVA GLP (Figures 5C and 5D). In contrast, no proliferation was seen in groups of mice given the non-specific control RPL6 GLP vaccine (Figures 5A–5D). To increase the sensitivity of this assay,³⁵ mice were analyzed as before at day 21, 56, and 131+ using 10-fold fewer donor T cells. CTV dilution in the spleen 10 days post transfer indicated antigen was still present 56 days post vaccination but had been cleared by day 131 (Figures 5E and S5). cDC1 cells were unlikely to be the source of this persistent antigen as depletion of cDC1

Figure 3. cDC1 are crucial for priming CD8⁺ T cell response to GLP vaccine

B6 (open circles) and XCR1-DTR mice (closed circles) were vaccinated with RPL6 GLP vaccine. To assess cDC1 function, these mice were either left untreated or were injected with DT every 2 days, starting 1 day before vaccination up to day 3 post vaccination. Untreated B6 and XCR1-DTR and unvaccinated B6 mice were also included.

(A–C) Representative FACS plots (A) and absolute numbers of cDC1 (CD11c⁺ MHC II⁺ XCR1⁺ CD172^{α-}) and cDC2 (CD11c⁺ MHC II⁺ XCR1⁻ CD172^{α+}) subsets in the spleen (B) and liver (C) 5 days after vaccination. Mean ± SEM.

(D–F) Some mice were rested for >21 days and the memory T cell responses assessed by flow cytometry. (D and E) The number of RPL6-specific (tet⁺) (Trm [black; CD8⁺ CD44⁺ CD69⁺ CD62L⁻], Tem [gray; CD8⁺ CD44⁺ CD69⁻ CD62L⁻], and Tcm [white; CD8⁺ CD44⁺ CD69⁻ CD62L⁺]) cells in the spleen (D) and liver (E). (F) The number of RPL6-specific CD8⁺ liver Trm cells in individual mice (circles). Mean ± SEM. Data are pooled from two independent experiments ($n = 8-10$ mice per group).

(G–L) The number of NKT cells (G and H), mean fluorescent intensity (MFI) of CD69 on NKT cells (I and J), and the percentage of NK1.1⁺-expressing NKT cells (K and L) in the spleen (upper row) and liver (lower row) at day 5 post vaccination. Mean ± SEM. Data in (B), (C), and (G)–(L) are pooled from two independent experiments ($n = 4-5$ mice per group). Indicated groups in (B), (C), (F), and (G)–(L) were log transformed and compared using an unpaired t test or Mann-Whitney U test. ns, not significant; * $p < 0.05$, ** $p < 0.01$, *** $p < 0.001$, **** $p < 0.0001$.

Figure 4. The role of GLP-derived antigen and inflammation in formation and long-term survival of liver Trm cells

B6 mice were i.v. injected with 5×10^6 *in vitro*-activated OT-I cells. One day later, recipient mice were vaccinated with OVA GLP, RPL6 GLP, α -GalCer (α GC), or left untreated (NIL) and then examined for memory OT-I cell responses in the liver and spleen 30 days later.

(A) Representative FACS plots showing Trm (CD69⁺ CD62L⁻), Tem (CD69⁻ CD62L⁻), and Tcm (CD69⁻ CD62L⁺) cells within the CD44⁺ OT-I cell population in the liver.

(B–D) (B) The number of OT-I Trm cells in the liver. Mean ± SEM. The number of OT-I Trm (black), Tem (gray), and Tcm (white) cells in the liver (C) and spleen (D). Data are pooled from two to three independent experiments ($n = 10-15$ mice per group).

(E–G) B6 mice were i.v. injected with 5×10^6 *in vitro*-activated OT-I cells alone (NIL), or 1 day later vaccinated with OVA SPAAC conjugated GLP vaccines containing either a β -ManCer (β MC-OVA GLP) or an α -GalCer adjuvant (α GC-OVA GLP) and then examined for memory OT-I responses in the liver and spleen 30 days later. (E) The number of OT-I Trm (CD8⁺ CD44⁺ CD69⁺ CD62L⁻) cells in the liver. Mean ± SEM. The number of OT-I Trm (black), Tem (gray; CD8⁺ CD44⁺ CD69⁻ CD62L⁻), and Tcm (white; CD8⁺ CD44⁺ CD69⁻ CD62L⁺) cells in the liver (F) and spleen (G). Data are pooled from two independent experiments ($n = 9-10$ mice per group).

(H) OT-I Trm numbers measured at various time points post vaccination, with estimated half-life of liver Trm cells ($t_{1/2}$) indicated for each group. Mean ± SD. Data for each group in each indicated

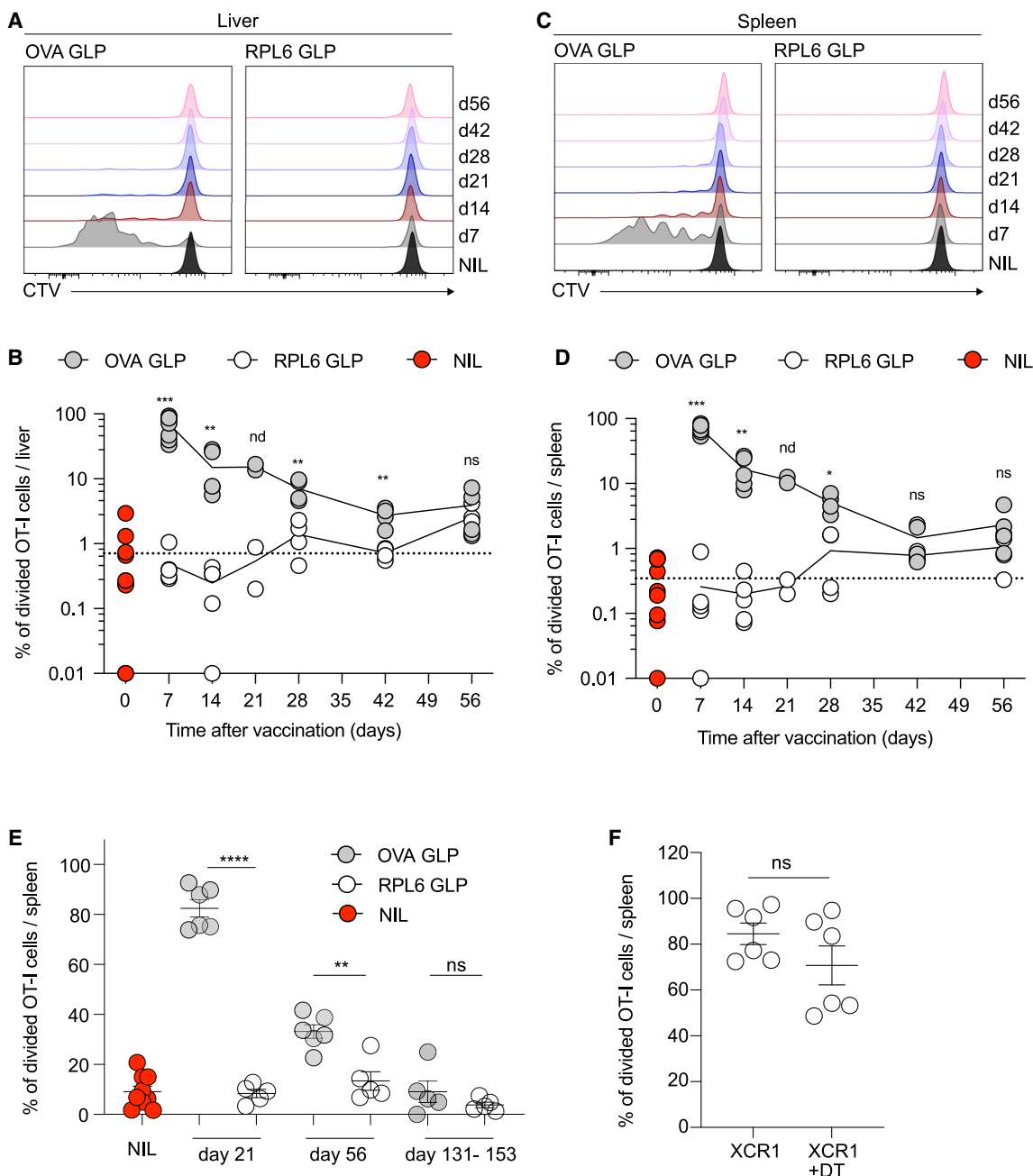


Figure 5. Long-term persistence of residual antigen in tissues after vaccination with GLP

(A–E) B6 mice were pre-immunized i.v. with OVA GLP or RPL6 GLP vaccine. At various indicated time points, $1\text{--}2 \times 10^6$ (A–D) or 1×10^5 (E) naive CTV-labeled OT-I cells were transferred into vaccinated mice and OT-I cell proliferation was examined by flow cytometry 2 (A–D) or 10 days (E) later. (A–D) Representative histograms (A and C) and the percentage of divided OT-I cells (B, D, and E) in the liver and spleen.

(F) XCR1-DTR mice were pre-immunized i.v. with OVA GLP. At day 20, half the mice were treated with DT to deplete cDC1. The following day, 1×10^5 naive CTV-labeled OT-I cells were transferred into vaccinated mice and OT-I cell proliferation was examined by flow cytometry in the spleen 10 days later.

NIL indicates unvaccinated mice that received naive CTV-labeled OT-I cells. Circles represent individual mice. Data are pooled from two to four independent experiments ($n = 4\text{--}9$ mice per group for each time point) except for day 21 (A–D) with only one experiment ($n = 2$ mice). For each indicated time point, OVA GLP (B, D, and E) was compared with RPL6 GLP using an unpaired t test or Mann-Whitney U test. No statistics were performed on day 21 data from (B) (denoted as "nd"). Zero values in (B) and (D) were given an arbitrary value of 0.01 for representation on the log-scale y axis. ns, not significant; * $p < 0.05$; ** $p < 0.01$; *** $p < 0.001$; **** $p < 0.0001$.

20 days post vaccination did not influence the proliferative capacity of donor OT-I cells transferred the next day and then assessed 10 days later (Figure 5F). Combined, these data suggest that antigen, in a form recognized by naive T cells, persists for at least 56 days after immunization with GLP vaccines, but that cDC1 are unlikely to be the population presenting this antigen.

A long interval between vaccinations is required for efficient homologous boosting with GLP vaccines

Intravenous immunization with GLP vaccines is clearly complex, with cDC1 dependence and contributions during T cell priming as well as post activation. We have previously shown that mice can be boosted by the RPL6 GLP vaccine if re-immunized on day 30 post priming,¹² but we had not explored the effect of varying this time interval. To assess this variable, B6 mice were vaccinated with the RPL6 GLP vaccine and then boosted with the same vaccine at different time points, ranging from day 9 to day 60. Then, 30 days after boosting, the numbers of endogenous RPL6-specific liver Trm cells were examined (Figure 6A). This study revealed significantly higher numbers of Trm cells in mice with long prime-boost intervals (30 or 60 days), with the highest Trm cell number induced after 60 days. In contrast, homologous prime-boost immunizations at short intervals (9, 14, or 23 days) failed to boost liver Trm cell numbers. To test the protective function of liver Trm cells after different booster intervals, mice from each group were first challenged with 200 PbA sporozoites, and then, if protected, were re-challenged with 3,000 PbA sporozoites. This showed virtually all mice were protected from both challenges, likely due to the large numbers of liver Trm cells in these mice that exceed the protective threshold⁶ (Figure 6B). To determine if boosting did in fact increase protective immunity, mice receiving one or two doses (30-day interval) of RPL6 GLP vaccine were challenged with 30,000 luciferase-expressing sporozoites and parasite burden (luciferase activity) in the liver was assessed by IVIS imaging 42 h later. While a single dose of RPL6 GLP showed an average lower parasite burden relative to naive mice, this difference was not significant. In contrast, priming followed by a booster vaccine led to a large reduction in parasite burden that was significantly greater than both naive mice and those given a single vaccination (Figure 6C). Together, these data showed that a longer homologous prime-boost interval resulted in improved liver Trm cell numbers and protection from challenge with very high doses of sporozoites. To assess whether a 60-day prime-boost interval would be effective with antigens other than RPL6, new groups of mice were primed with OVA GLP and then boosted with the same vaccine after 60 days. Examination of liver Trm cells in these mice reveal effective boosting by this regime (Figures 6D–6F).

Heterologous boosting reduces the required prime-boost interval

NKT cells are known to become hyporesponsive after α -GalCer-induced activation, displaying impaired inflammatory cytokine production and blunted proliferation upon restimulation with α -GalCer.^{23,24} Given the reliance of GLP vaccine-induced CD8⁺ T cell responses on NKT cells,¹² we hypothesized that the failure to boost liver Trm responses early after GLP vaccination may be associated with NKT cell anergy. Enumeration of

liver NKT cells at different time points after immunization with RPL6 GLP vaccine showed minimal changes in cell numbers at days 9–23, with a slight numerical decline at days 30 and 60 compared to naive or day 9 (Figures S6A and S6B). Phenotypic analysis of liver NKT cells after GLP vaccination showed down-regulated NK1.1 expression (Figure S6C) and enhanced PD-1 expression (Figure S6D), indicating NKT cell activation, and these phenotypic changes remained throughout the course of analysis. There appeared to be a modest recovery in some phenotypic characteristics of liver NKT cells over time after GLP vaccination, but whether this change was sufficient to explain the improved secondary boosting of liver Trm responses when boosting was delayed by >30 days was unclear. To address whether boosting could be achieved earlier if independent of NKT cells, we used a previously established immunization approach: RPL6-targeted anti-Clec9A antibody and CpG 2006-21798 adjuvant (hereafter this combination is referred to as CC) as a vaccine booster.⁷ CD1d^{-/-} mice, which lack NKT cells, were able to efficiently generate liver Trm cells by this method (Figure 7A), indicating this vaccine generated immunity independent of NKT cell participation. To examine heterologous boosting independent of NKT cells, B6 mice were primed with RPL6 GLP vaccine and then boosted with CC at different time points after priming, with liver Trm cell numbers enumerated >30 days later (Figure 7B). This showed a significant boost in liver Trm cell responses when CC was administered as early as day 9 after GLP priming, with no significant improvement seen by further delaying boosting to day 30 (Figure 7B). These results showed that GLP-induced CD8⁺ T cells were intrinsically responsive to secondary boosting during the early phase of the immune response and that booster immunizations that bypass NKT cell activation could shorten the interval required for secondary amplification of GLP-induced liver Trm cell responses.

DISCUSSION

Here we dissect the mechanisms underlying the effective generation of long-lived liver Trm cells by GLP vaccines. In response to i.v. injection of GLP vaccines, CD8⁺ T cells underwent rapid activation and began to proliferate as early as day 1 in the spleen and liver-draining lymph nodes. Although i.v. RAS vaccination can similarly induce CD8⁺ T cell activation 24 h after vaccination, CD8⁺ T cell proliferation was not evident until day 2.¹⁵ The more rapid response to GLP vaccines is likely related to their capacity to quickly access lymphoid tissues and provide high doses of specific antigen for activation of T cells and α -GalCer for activation of large numbers of NKT cells that efficiently help this response. In contrast, RAS vaccination would require sporozoite migration to lymphoid tissue or the liver, dendritic cell capture of antigen, and then stimulation of naive specific helper T cells before proliferation of CD8⁺ T cells could begin. The initiation of a CD8⁺ T cell response is critically dependent on XCR1⁺ cDC1, confirming our previous report showing a suboptimal endogenous CD8⁺ T cell response to the GLP vaccine in *Batf3*^{-/-} mice.²² Given Trm cells account for the majority (80%–90%) of memory T cells induced by GLP vaccines in the liver, cDC1 may play a specialized role in priming and imprinting Trm differentiation fate on the responding CD8⁺ T cells. In

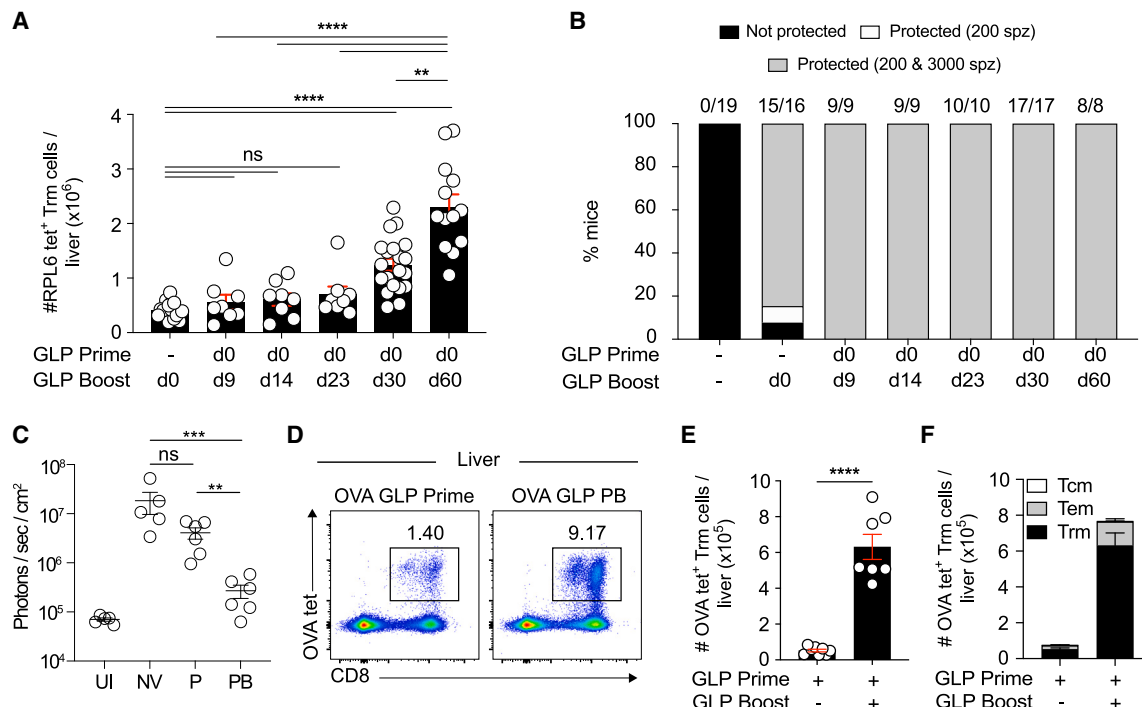


Figure 6. An interval of 60 days between prime and boost with GLP vaccine is highly effective for liver Trm cell boosting

B6 mice received one or two doses of RPL6 GLP vaccine at various indicated time intervals (9–60 days) with boosting aligned to the same day. 30 days after the last immunization, RPL6 tetramer (*tet*)⁺ memory CD8⁺ T cells in the livers and spleens of vaccinated mice were assessed by flow cytometry.

(A) The number of RPL6-specific CD8⁺ liver Trm cells. Mean ± SEM. Data are pooled from two to five independent experiments ($n = 8$ –20 mice per group). Data were log transformed and compared by the one-way ANOVA with Tukey's multiple comparison test. Separate cohorts of naive and vaccinated mice were challenged with 200 PbA sporozoites 1 month after the last immunization, and sterile protection was assessed by monitoring blood-stage parasitemia up to day 12 post infection. Mice showing no parasitemia were recorded as protected and were re-challenged with 3,000 PbA sporozoites 21 days after the first challenge and monitored for parasitemia for 13 days.

(B) Percentage of mice that were unprotected (black), protected from challenge with 200 PbA sporozoites (white), or protected against both 200 and 3,000 sporozoite challenges (gray). Numbers above bars indicate the number of mice that were protected against the initial 200-sporozoite challenge over total number of mice challenged. Data are pooled from two to four independent experiments ($n = 8$ –19 mice per group).

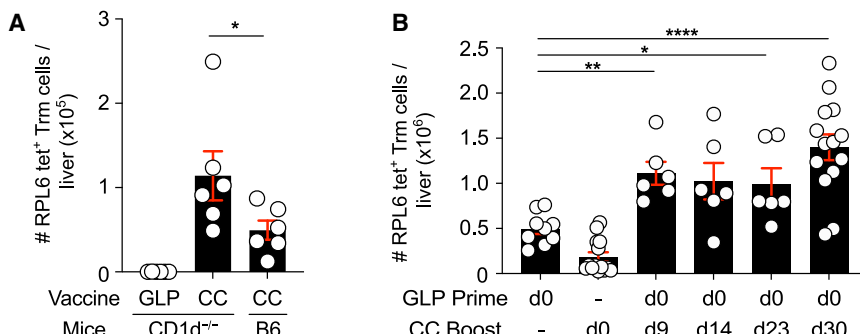
(C) B6 mice received one (P) or two doses (PB, 30-day interval) of RPL6 GLP. 30 days after the last immunization, mice were challenged with 30,000 luciferase sporozoites and imaged at 42 h by IVIS. Additional groups of imaged mice included uninfected (UI) mice and naive mice challenged with luciferase sporozoites (NV). Counts were log transformed and compared by one-way ANOVA with Sidak correction.

(D–F) B6 mice received one or two doses of OVA GLP vaccine given at a 60-day interval and were assessed for OVA-tetramer (*tet*)⁺ CD8⁺ T cells in the livers by flow cytometry 30 days later. (D) Representative flow cytometry plots of OVA-tet⁺ CD8⁺ T cells in the liver. (E) The number of OVA-specific Trm (CD8⁺ CD44⁺ CD69⁺ CD62L⁻) cells in the liver. Mean ± SEM. Data were log transformed and compared by an unpaired *t* test. (F) The number of OVA-specific Trm (black), Tem (gray; CD8⁺ CD44⁺ CD69⁻ CD62L⁻), and Tcm (white, CD8⁺ CD44⁺ CD69⁻ CD62L⁺) cells in the liver. Data are pooled from two independent experiments ($n = 7$ –8 mice per group). ns, not significant; ** $p < 0.01$; *** $p < 0.001$; **** $p < 0.0001$.

support of this idea, cDC1 cells have been implicated in generating memory precursor cells that are efficiently poised to form Trm cells, but not circulating memory T cells, in the skin and lung after viral infections.³⁶ Such a requirement for cDC1 was linked to their cross-presentation ability and the provision of IL-12, IL-15, and CD24 during priming,³⁶ but here we show that IL-12p40 is not required for liver Trm cell formation after GLP vaccination. In contrast to the CD8⁺ T cell response, we found that cDC1 cells were dispensable for NKT cell activation after priming with GLP vaccines, suggesting that NKT cells may be stimulated by cells in addition to cDC1. This result was supported by another recent study using hepatitis B virus GLPs.³⁷ However, it should be noted that, in the absence of cDC1 cells, induction of IL-12p70 (a typical downstream

response to NKT cell activation) was lost, suggesting NKT cells activated in this setting are compromised.³⁸ Further work is required to dissect the role of other CD1d-expressing APCs, such as cDC2, marginal zone macrophages, liver Kupffer cells, and B cells^{39–41} in presenting GLP-derived α -GalCer.

Using the adoptive transfer model of *in vitro*-activated CD8⁺ T cells, we provided evidence that seeding of liver Trm cells can be improved by exposure to inflammation or, to a lesser extent, antigen alone, although a combination of both is most effective. These results agree with previous reports showing liver-associated inflammation and antigen presentation can boost differentiation of effector T cells into liver Trm cells.¹⁶ IFN- γ was shown to contribute to the non-cognate inflammatory component that increased liver Trm cells in this adoptive transfer



CC at the indicated time points. The number of RPL6-specific Trm (CD8⁺ CD44⁺ CD69⁺ CD62L⁻) cells in the liver 30 days after vaccination. Data were pooled from two to four independent experiments ($n = 6$ –14 mice per group).

(A and B) Mean \pm SEM. Data were log transformed and compared using the one-way ANOVA with Tukey's multiple comparison test. In (B) the CC group was excluded from the analysis. * $p < 0.05$, ** $p < 0.01$, *** $p < 0.0001$.

model (Figure S4A). Interestingly, however, blocking IFN- γ had no effect in mice vaccinated normally with an RPL6 GLP when blocked for the first 3 days post vaccination. While reasons for this discrepancy are unexplained, it may relate to temporal differences in IFN- γ blockade. While normal vaccination examined blocking of naive T cells in the first 3 days of priming, the adoptive transfer system examined blocking of activated cells 4 days post priming *in vitro*. Extending from the observation that exposure to both antigen and inflammatory signals contribute to increased liver Trm cell numbers post activation, we showed that the longevity of liver Trm cells could also be regulated by post-activation antigenic signals. When *in vitro*-activated OT-I cells are transferred into mice subsequently injected with the OVA GLP vaccine and allowed to form liver Trm cells, these cells were longer lived than those without secondary vaccine-associated signals or with antigen-non-specific signals alone (RPL6 GLP vaccine). The increase in half-life was \sim 2-fold, increasing from 28 to 58 days, but still substantially shorter than the 8-fold greater half-life (236 days) of Trm cells primed directly by the GLP vaccine. A related increase in half-life has been reported for skin Trm cells⁴² where antigen-experienced skin Trm cells (induced by local viral infection) displayed a survival advantage over bystander counterparts (induced by DNFB-induced inflammation) owing to their enhanced capacity to compete for limiting survival factors in the local tissue microenvironment. The molecular mechanisms underlying this effect were not well understood but were thought to be associated with epigenetic modifications within the skin Trm cells. The GLP vaccine's dependence on post-priming antigenic signals for the 2-fold increase in Trm cell half-life suggested secondary antigenic signals provided by persistent antigen in the liver may contribute to liver Trm cell survival. This notion was raised in a previous study that showed that long-term persistence of lung Trm cells was achieved by recurring exposure to antigenic signals in the lung.⁴³ In our case, kinetics studies showed that antigen persisted in the liver and spleen for at least 56 days after GLP vaccination but cDC1 cells were unlikely to be acting as the antigen depot. Therefore, it is tempting to speculate that certain hepatic APCs, such as liver sinusoidal endothelial cells, other

Figure 7. Booster immunization with RPL6-targeted anti-Clec9A antibody and CpG adjuvant accelerates the boosting of liver Trm cell responses primed by the GLP vaccine

(A) B6 or CD1d^{-/-} mice were vaccinated i.v. with either RPL6 GLP vaccine or anti-Clec9A-NVF antibody and CpG 2006-21798 adjuvant (CC). The number of RPL6-tetramer (tet)⁺ Trm (CD8⁺ CD44⁺ CD69⁺ CD62L⁻) cells were then assessed in the liver 30 days after vaccination. Data are pooled from two independent experiments ($n = 6$ mice per group).

(B) B6 mice were immunized i.v. with the RPL6 GLP vaccine or CC alone, or were immunized i.v. with the RPL6 GLP vaccine and then boosted with

DCs, or Kupffer cells, may serve as an antigen depot in the liver to support liver Trm cell maintenance. Whatever the case, this antigen depot only partially explains the capacity of GLP vaccines to generate long-lived Trm cells as the half-life of Trm cells derived from transferred activated T cells was only increased to 58 days in the presence of antigen, much less than the 236-day half-life of liver Trm cells generated directly by GLP vaccination. This difference implies a major component of lifespan may be programmed during priming, aligning with the possibility of epigenetic or other gene-expression changes as raised previously.⁴²

Prime-boost immunization is a common strategy used in the vaccine field to address waning immunity. In the case of malaria liver-stage infections, long-term sterile immunity can be achieved by generating sufficiently high numbers of protective liver Trm cells above the protective threshold. Our previous study demonstrated the feasibility of boosting liver Trm responses by administrating two doses of a GLP vaccine with a 30-day interval.¹² Here, we extended this finding by demonstrating that optimal boosting of liver Trm cell numbers can be achieved by either homologous boosting with GLP vaccines or by heterologous prime-boost immunization with GLP priming followed by RPL6-targeted anti-Clec9A antibody and CpG 2006-21798 adjuvant boosting. From a clinical perspective, a heterologous prime-boost regimen may be more advantageous because it could be achieved in a significantly shorter time interval (i.e., 9 days). The necessity for prolonged prime-boost intervals (>30 days) for the homologous regimen to improve secondary liver Trm cell responses likely reflects the hypo-responsiveness of NKT cells, rather than unresponsiveness of CD8⁺ T cells themselves, to secondary antigenic stimulation early after GLP priming. This can be supported by (1) mounting evidence from previous studies showing the induction of long-term NKT cell anergy by α -GalCer,^{23,24,44} (2) our observation that NKT cells partially recovered phenotypically at day 60 after GLP vaccination, and (3) the fact that heterologous Clec9A boosting can increase liver Trm cell responses much earlier, and in a non-NKT cell-dependent fashion. Overall, our findings demonstrate how timing between priming and boosting can influence vaccine efficacy and

highlight the value of using an NKT cell-independent booster agent to complement primary immunization with an α -GalCer-formulated vaccine for optimal and rapid boosting of vaccine-induced immunity.

Translating these findings into human therapies is highly feasible as processing of GLP vaccines by cDC1 releases the prodrug glycolipid, which spontaneously rearranges to form α -GalCer. α -GalCer has been safely utilized in primates⁴⁵ and humans⁴⁶ in soluble form and has shown some efficacy in human cancer clinical trials when pulsed on DCs.^{47–49} More effective forms of α -GalCer have also been developed for humans, (e.g., ABX196), and translational approaches have the potential to incorporate these modified forms of α -GalCer into this GLP format.

In summary, we examined the developmental requirements of long-lived liver Trm cells in the context of GLP vaccination. We revealed that the underlying immune process is highly dependent on cDC1 priming and antigen/inflammation encounter during seeding in the liver. Furthermore, we highlight that primary immunization with α -GalCer-based vaccines should consider using a non-NKT cell-dependent vaccine as a booster to allow for a rapid boosting of vaccine-induced immunity.

Limitations of the study

While we demonstrated that antigen persisted for at least 56 days following GLP vaccination, as shown by the proliferation of adoptively transferred naive OT-I cells, it remains unclear whether memory CD8⁺ T cells would respond to the persistent antigen in the same way as their naive counterparts. Additionally, although prime-boost immunizations increased the number of liver Trm cells, the effect of vaccine booster on the duration of antigen persistence and/or the lifespan of liver Trm cells remains unknown, warranting further investigation.

RESOURCE AVAILABILITY

Lead contact

Further information and requests for resources and reagents should be directed to and will be fulfilled by the lead contact, Dr. Lauren Holz (lauren.holz@unimelb.edu.au).

Materials availability

There are restrictions to the availability of GLP vaccines due to material transfer agreements and shipping costs.

Data and code availability

- All data reported in this paper will be shared by the [lead contact](#) upon request.
- This paper does not report original code.
- Any additional information required to reanalyze the data reported in this paper is available from the [lead contact](#) upon request.

ACKNOWLEDGMENTS

We thank Calvin Xu and Dale Godfrey (Doherty Institute, University of Melbourne) for providing the CD1d tetramers. We also thank the staff from the flow cytometry and bioresources platforms at the Doherty Institute for their assistance. This work was supported by funding from the National Health and Medical Research Council of Australia (NHMRC). W.R.H. and L.E.H. were supported by NHMRC 2012701, W.R.H. by NHMRC 1154457, S.G. by NHMRC SRF 1159272, M.H.L. by NHMRC 2020613, G.I.M. by NHMRC 2016391, and T.K. by JP22H05187 and Takeda Science Foundation. Additional support was provided by the National New Zealand Ministry of Business

Innovation and Employment (contract RTVU1603 to Victoria University of Wellington) and the New Zealand Health Research Council (contract HRC-20/569 to Victoria University of Wellington and HRC14/1003 Independent Research Organisation Fund to the Malaghan Institute).

AUTHOR CONTRIBUTIONS

Conceptualization, I.F.H., W.R.H., G.F.P., L.E.H., and Y.C.C.; methodology, S.L.D., M.H.L., I.C., G.I.M., D.S.L., T.K., S.G., I.F.H., B.J.C., W.R.H., G.F.P., and L.E.H.; formal analysis, Y.C.C., S.L.D., W.R.H., and L.E.H.; investigation, Y.C.C., S.L.D., S.L., M.G., Z.G., A.L., T.P., D.H., S.A.R., P.S.T., K.M.T., D.J., A.C., and M.N.D.M.; resources, S.L.D., S.A.R., P.S.T., K.M.T., R.J.A., D.J., A.C., M.H.L., I.C., G.I.M., D.S.L., T.S., S.G., and I.F.H.; writing – original draft, Y.C.C., W.R.H., and L.E.H.; writing – review & editing, Y.C.C., S.L.D., P.S.T., K.M.T., M.H.L., G.I.M., T.S., S.G., I.F.H., B.J.C., W.R.H., G.F.P., and L.E.H.; visualization, Y.C.C. and L.E.H.; supervision, M.H.L., I.C., L.B., G.I.M., S.G., B.J.C., D.S.L., I.F.H., W.R.H., G.F.P., and L.E.H.; project administration, I.F.H., W.R.H., G.F.P., and L.E.H.; funding acquisition, I.F.H., G.F.P., and W.R.H.

DECLARATION OF INTERESTS

G.F.P. and I.F.H. have been chief technical officer and chief scientific officer, respectively, of biotech start-up Avalia Immunotherapies Limited, and W.R.H. was a member of its Scientific Advisory Board. Avalia holds exclusive, worldwide license to patents related to aspects of the chemical design reported here. Avalia partially funded the study. W.R.H., I.F.H., L.E.H., B.J.C., and G.F.P. are inventors on patent application (WO2020231274) submitted by Victoria University of Wellington, Malcorp Biodiscoveries Limited, and Victoria Link Limited that covers the production of tissue-resident memory T cells with GLP vaccines. M.H.L., K.M.T., and I.C. are inventors on patents relating to Clec9A antibodies.

STAR METHODS

Detailed methods are provided in the online version of this paper and include the following:

- KEY RESOURCES TABLE
- EXPERIMENTAL MODEL AND STUDY PARTICIPANT DETAILS
- METHOD DETAILS
 - Vaccine manufacture
 - T cell transfer
 - Vaccination
 - *In vitro* OT-I cell activation
 - *In vivo* cDC1 depletion
 - Organ harvest and processing
 - FACS staining and analysis
 - Malaria challenge
 - IVIS imaging
- QUANTIFICATION AND STATISTICAL ANALYSIS

SUPPLEMENTAL INFORMATION

Supplemental information can be found online at <https://doi.org/10.1016/j.celrep.2025.115295>.

Received: March 7, 2024

Revised: October 12, 2024

Accepted: January 20, 2025

Published: February 12, 2025

REFERENCES

1. WHO (2023). World Malaria Report 2023 (World Health Organization). <https://www.who.int/teams/global-malaria-programme/reports/world-malaria-report-2023>.

2. Holz, L.E., Fernandez-Ruiz, D., and Heath, W.R. (2016). Protective immunity to liver-stage malaria. *Clin. Transl. Immunology* 5, e105. <https://doi.org/10.1038/cti.2016.60>.
3. Datoo, M.S., Natama, H.M., Somé, A., Bellamy, D., Traoré, O., Rouamba, T., Tahita, M.C., Ido, N.F.A., Yameogo, P., Valia, D., et al. (2022). Efficacy and immunogenicity of R21/Matrix-M vaccine against clinical malaria after 2 years' follow-up in children in Burkina Faso: a phase 1/2b randomised controlled trial. *Lancet Infect. Dis.* 22, 1728–1736. [https://doi.org/10.1016/S1473-3099\(22\)00442-X](https://doi.org/10.1016/S1473-3099(22)00442-X).
4. Schofield, L., Villaquiran, J., Ferreira, A., Schellekens, H., Nussenzweig, R., and Nussenzweig, V. (1987). Gamma interferon, CD8+ T cells and antibodies required for immunity to malaria sporozoites. *Nature* 330, 664–666. <https://doi.org/10.1038/330664a0>.
5. Weiss, W.R., Sedegah, M., Beaudoin, R.L., Miller, L.H., and Good, M.F. (1988). CD8+ T cells (cytotoxic/suppressors) are required for protection in mice immunized with malaria sporozoites. *Proc. Natl. Acad. Sci. USA* 85, 573–576.
6. Schmidt, N.W., Podyminogin, R.L., Butler, N.S., Badovinac, V.P., Tucker, B.J., Bahjat, K.S., Lauer, P., Reyes-Sandoval, A., Hutchings, C.L., Moore, A.C., et al. (2008). Memory CD8 T cell responses exceeding a large but definable threshold provide long-term immunity to malaria. *Proc. Natl. Acad. Sci. USA* 105, 14017–14022. <https://doi.org/10.1073/pnas.0805452105>.
7. Fernandez-Ruiz, D., Ng, W.Y., Holz, L.E., Ma, J.Z., Zaid, A., Wong, Y.C., Lau, L.S., Mollard, V., Cozijnsen, A., Collins, N., et al. (2016). Liver-resident memory CD8+ T cells form a front-line defense against malaria liver-stage infection. *Immunity* 45, 889–902.
8. Ganley, M., Holz, L.E., Minnelli, J.J., de Menezes, M.N., Burn, O.K., Poa, K.C.Y., Draper, S.L., English, K., Chan, S.T.S., Anderson, R.J., et al. (2023). mRNA vaccine against malaria tailored for liver-resident memory T cells. *Nat. Immunol.* 24, 1487–1498. <https://doi.org/10.1038/s41590-023-01562-6>.
9. Lefebvre, M.N., Surette, F.A., Anthony, S.M., Vijay, R., Jensen, I.J., Pewe, L.L., Hancox, L.S., Van Braeckel-Budimir, N., van de Wall, S., Urban, S.L., et al. (2021). Expedited recruitment of circulating memory CD8 T cells to the liver facilitates control of malaria. *Cell Rep.* 37, 109956. <https://doi.org/10.1016/j.celrep.2021.109956>.
10. Gola, A., Silman, D., Walters, A.A., Sridhar, S., Uderhardt, S., Salman, A.M., Halbroth, B.R., Bellamy, D., Bowyer, G., Powson, J., et al. (2018). Prime and target immunization protects against liver-stage malaria in mice. *Sci. Transl. Med.* 10, eaap9128. <https://doi.org/10.1126/scitranslmed.aap9128>.
11. Olsen, T.M., Stone, B.C., Chuenchob, V., and Murphy, S.C. (2018). Prime-and-Trap Malaria Vaccination To Generate Protective CD8(+) Liver-Resident Memory T Cells. *J. Immunol.* 201, 1984–1993. <https://doi.org/10.4049/jimmunol.1800740>.
12. Holz, L.E., Chua, Y.C., de Menezes, M.N., Anderson, R.J., Draper, S.L., Compton, B.J., Chan, S.T.S., Mathew, J., Li, J., Kedzierski, L., et al. (2020). Glycolipid-peptide vaccination induces liver-resident memory CD8(+) T cells that protect against rodent malaria. *Sci. Immunol.* 5, eaaz8035. <https://doi.org/10.1126/sciimmunol.aaz8035>.
13. Epstein, J.E., Tewari, K., Lyke, K.E., Sim, B.K.L., Billingsley, P.F., Laurens, M.B., Gunasekera, A., Chakravarty, S., James, E.R., Sedegah, M., et al. (2011). Live attenuated malaria vaccine designed to protect through hepatic CD8(+) T cell immunity. *Science* 334, 475–480. <https://doi.org/10.1126/science.1211548>.
14. Seder, R.A., Chang, L.J., Enama, M.E., Zephir, K.L., Sarwar, U.N., Gordon, I.J., Holman, L.A., James, E.R., Billingsley, P.F., Gunasekera, A., et al. (2013). Protection against malaria by intravenous immunization with a non-replicating sporozoite vaccine. *Science* 341, 1359–1365. <https://doi.org/10.1126/science.1241800>.
15. Lau, L.S., Fernandez-Ruiz, D., Mollard, V., Sturm, A., Neller, M.A., Cozijnsen, A., Gregory, J.L., Davey, G.M., Jones, C.M., Lin, Y.H., et al. (2014).
- CD8+ T cells from a novel T cell receptor transgenic mouse induce liver-stage immunity that can be boosted by blood-stage infection in rodent malaria. *PLoS Pathog.* 10, e1004135. <https://doi.org/10.1371/journal.ppat.1004135>.
16. Holz, L.E., Prier, J.E., Freestone, D., Steiner, T.M., English, K., Johnson, D.N., Mollard, V., Cozijnsen, A., Davey, G.M., Godfrey, D.I., et al. (2018). CD8(+) T Cell Activation Leads to Constitutive Formation of Liver Tissue-Resident Memory T Cells that Seed a Large and Flexible Niche in the Liver. *Cell Rep.* 25, 68–79.e4. <https://doi.org/10.1016/j.celrep.2018.08.094>.
17. Ishizuka, A.S., Lyke, K.E., DeZure, A., Berry, A.A., Richie, T.L., Mendoza, F.H., Enama, M.E., Gordon, I.J., Chang, L.J., Sarwar, U.N., et al. (2016). Protection against malaria at 1 year and immune correlates following PfSPZ vaccination. *Nat. Med.* 22, 614–623. <https://doi.org/10.1038/nm.4110>.
18. Lyke, K.E., Ishizuka, A.S., Berry, A.A., Chakravarty, S., DeZure, A., Enama, M.E., James, E.R., Billingsley, P.F., Gunasekera, A., Manoj, A., et al. (2017). Attenuated PfSPZ Vaccine induces strain-transcending T cells and durable protection against heterologous controlled human malaria infection. *Proc. Natl. Acad. Sci. USA* 114, 2711–2716. <https://doi.org/10.1073/pnas.1615324114>.
19. Sissoko, M.S., Healy, S.A., Katile, A., Omaswa, F., Zaidi, I., Gabriel, E.E., Kamate, B., Samake, Y., Guindo, M.A., Dolo, A., et al. (2017). Safety and efficacy of PfSPZ Vaccine against Plasmodium falciparum via direct venous inoculation in healthy malaria-exposed adults in Mali: a randomised, double-blind phase 1 trial. *Lancet Infect. Dis.* 17, 498–509. [https://doi.org/10.1016/S1473-3099\(17\)30104-4](https://doi.org/10.1016/S1473-3099(17)30104-4).
20. Sissoko, M.S., Healy, S.A., Katile, A., Zaidi, I., Hu, Z., Kamate, B., Samake, Y., Sissoko, K., Mwakingwe-Omari, A., Lane, J., et al. (2022). Safety and efficacy of a three-dose regimen of Plasmodium falciparum sporozoite vaccine in adults during an intense malaria transmission season in Mali: a randomised, controlled phase 1 trial. *Lancet Infect. Dis.* 22, 377–389. [https://doi.org/10.1016/S1473-3099\(21\)00332-7](https://doi.org/10.1016/S1473-3099(21)00332-7).
21. Speir, M., Authier-Hall, A., Brooks, C.R., Farrand, K.J., Compton, B.J., Anderson, R.J., Heiser, A., Osmond, T.L., Tang, C.W., Berzofsky, J.A., et al. (2017). Glycolipid-peptide conjugate vaccines enhance CD8(+) T cell responses against human viral proteins. *Sci. Rep.* 7, 14273. <https://doi.org/10.1038/s41598-017-14690-5>.
22. Compton, B.J., Farrand, K.J., Tang, C.W., Osmond, T.L., Speir, M., Authier-Hall, A., Wang, J., Ferguson, P.M., Chan, S.T.S., Anderson, R.J., et al. (2019). Enhancing T cell responses and tumour immunity by vaccination with peptides conjugated to a weak NKT cell agonist. *Org. Biomol. Chem.* 17, 1225–1237. <https://doi.org/10.1039/c8ob02982b>.
23. Uldrich, A.P., Crowe, N.Y., Kyparissoudis, K., Pellicci, D.G., Zhan, Y., Lew, A.M., Bouillet, P., Strasser, A., Smyth, M.J., and Godfrey, D.I. (2005). NKT cell stimulation with glycolipid antigen in vivo: costimulation-dependent expansion, Bim-dependent contraction, and hyporesponsiveness to further antigenic challenge. *J. Immunol.* 175, 3092–3101.
24. Parekh, V.V., Wilson, M.T., Olivares-Villagómez, D., Singh, A.K., Wu, L., Wang, C.R., Joyce, S., and Van Kaer, L. (2005). Glycolipid antigen induces long-term natural killer T cell energy in mice. *J. Clin. Invest.* 115, 2572–2583. <https://doi.org/10.1172/JCI24762>.
25. Valencia-Hernandez, A.M., Ng, W.Y., Ghazanfari, N., Ghilas, S., de Menezes, M.N., Holz, L.E., Huang, C., English, K., Naung, M., Tan, P.S., et al. (2020). A Natural Peptide Antigen within the Plasmodium Ribosomal Protein RPL6 Confers Liver TRM Cell-Mediated Immunity against Malaria in Mice. *Cell Host Microbe* 27, 950–962.e7. <https://doi.org/10.1016/j.chom.2020.04.010>.
26. Hildner, K., Edelson, B.T., Purtha, W.E., Diamond, M., Matsushita, H., Kohyama, M., Calderon, B., Schraml, B.U., Unanue, E.R., Diamond, M.S., et al. (2008). Batf3 deficiency reveals a critical role for CD8alpha+ dendritic

- cells in cytotoxic T cell immunity. *Science* 322, 1097–1100. <https://doi.org/10.1126/science.1164206>.
27. Ataide, M.A., Komander, K., Knöpper, K., Peters, A.E., Wu, H., Eickhoff, S., Gogishvili, T., Weber, J., Grafen, A., Kallies, A., et al. (2020). BATF3 programs CD8(+) T cell memory. *Nat. Immunol.* 21, 1397–1407. <https://doi.org/10.1038/s41590-020-0786-2>.
 28. Yamazaki, C., Sugiyama, M., Ohta, T., Hemmi, H., Hamada, E., Sasaki, I., Fukuda, Y., Yano, T., Nobuoka, M., Hirashima, T., et al. (2013). Critical roles of a dendritic cell subset expressing a chemokine receptor, XCR1. *J. Immunol.* 190, 6071–6082. <https://doi.org/10.4049/jimmunol.1202798>.
 29. Schenkel, J.M., Fraser, K.A., and Masopust, D. (2014). Cutting edge: resident memory CD8 T cells occupy frontline niches in secondary lymphoid organs. *J. Immunol.* 192, 2961–2964. <https://doi.org/10.4049/jimmunol.1400003>.
 30. Cossarizza, A., Chang, H.D., Radbruch, A., Abrignani, S., Addo, R., Akdis, M., Andrà, I., Andreata, F., Annunziato, F., Arranz, E., et al. (2021). Guidelines for the use of flow cytometry and cell sorting in immunological studies (third edition). *Eur. J. Immunol.* 51, 2708–3145. <https://doi.org/10.1002/eji.202170126>.
 31. Christian, D.A., Adams, T.A., 2nd, Shallberg, L.A., Phan, A.T., Smith, T.E., Abraha, M., Perry, J., Ruthel, G., Clark, J.T., Pritchard, G.H., et al. (2022). cDC1 coordinate innate and adaptive responses in the omentum required for T cell priming and memory. *Sci. Immunol.* 7, eabq7432. <https://doi.org/10.1126/sciimmunol.abq7432>.
 32. Hickman, H.D., Takeda, K., Skon, C.N., Murray, F.R., Hensley, S.E., Loomis, J., Barber, G.N., Bennink, J.R., and Yewdell, J.W. (2008). Direct priming of antiviral CD8+ T cells in the peripheral interfollicular region of lymph nodes. *Nat. Immunol.* 9, 155–165. <https://doi.org/10.1038/ni1557>.
 33. O'Konek, J.J., Illarionov, P., Khursigara, D.S., Ambrosino, E., Izhak, L., Castillo, B.F., Raju, R., Khalili, M., Kim, H.Y., Howell, A.R., et al. (2011). Mouse and human iNKT cell agonist beta-mannosylceramide reveals a distinct mechanism of tumor immunity. *J. Clin. Invest.* 121, 683–694. <https://doi.org/10.1172/JCI42314>.
 34. Robinson, S.A., Yau, J., Terabe, M., Berzofsky, J.A., Painter, G.F., Compton, B.J., and Larsen, D.S. (2020). Synthetic preparation and immunological evaluation of beta-mannosylceramide and related N-acyl analogues. *Org. Biomol. Chem.* 18, 2739–2746. <https://doi.org/10.1039/dob00223b>.
 35. Cockburn, I.A., Chen, Y.C., Overstreet, M.G., Lees, J.R., van Rooijen, N., Farber, D.L., and Zavala, F. (2010). Prolonged antigen presentation is required for optimal CD8+ T cell responses against malaria liver stage parasites. *PLoS Pathog.* 6, e1000877. <https://doi.org/10.1371/journal.ppat.1000877>.
 36. Iborra, S., Martínez-López, M., Khouili, S.C., Enamorado, M., Cueto, F.J., Conde-Garrrosa, R., Del Fresno, C., and Sancho, D. (2016). Optimal Generation of Tissue-Resident but Not Circulating Memory T Cells during Viral Infection Requires Crosspriming by DNLR-1(+) Dendritic Cells. *Immunity* 45, 847–860. <https://doi.org/10.1016/j.jimmuni.2016.08.019>.
 37. Mooney, A.H., Draper, S.L., Burn, O.K., Anderson, R.J., Compton, B.J., Tang, C., Farrand, K.J., Di Lucia, P., Ravà, M., Fumagalli, V., et al. (2024). Preclinical evaluation of therapeutic vaccines for chronic hepatitis B that stimulate antiviral activities of T cells and NKT cells. *JHEP Rep.* 6, 101038. <https://doi.org/10.1016/j.jhepr.2024.101038>.
 38. Anderson, R.J., Tang, C.W., Daniels, N.J., Compton, B.J., Hayman, C.M., Johnston, K.A., Knight, D.A., Gasser, O., Poyntz, H.C., Ferguson, P.M., et al. (2014). A self-adjuvanting vaccine induces cytotoxic T lymphocytes that suppress allergy. *Nat. Chem. Biol.* 10, 943–949. <https://doi.org/10.1038/nchembio.1640>.
 39. Beogradica, J.S., Stanic, A.K., Matsuki, N., Bour-Jordan, H., Bluestone, J.A., Thomas, J.W., Unutmaz, D., Van Kaer, L., and Joyce, S. (2005). Distinct roles of dendritic cells and B cells in Va14Ja18 natural T cell activation in vivo. *J. Immunol.* 174, 4696–4705. <https://doi.org/10.4049/jimmunol.174.8.4696>.
 40. Schmieg, J., Yang, G., Franck, R.W., Van Rooijen, N., and Tsuji, M. (2005). Glycolipid presentation to natural killer T cells differs in an organ-dependent fashion. *Proc. Natl. Acad. Sci. USA* 102, 1127–1132. <https://doi.org/10.1073/pnas.0408288102>.
 41. Barral, P., Sánchez-Niño, M.D., van Rooijen, N., Cerundolo, V., and Batista, F.D. (2012). The location of splenic NKT cells favours their rapid activation by blood-borne antigen. *EMBO J.* 31, 2378–2390. <https://doi.org/10.1038/emboj.2012.87>.
 42. Hirai, T., Yang, Y., Zenke, Y., Li, H., Chaudhri, V.K., De La Cruz Diaz, J.S., Zhou, P.Y., Nguyen, B.A., Bartholin, L., Workman, C.J., et al. (2021). Competition for Active TGFbeta Cytokine Allows for Selective Retention of Antigen-Specific Tissue- Resident Memory T Cells in the Epidermal Niche. *Immunity* 54, 84–98.e85. <https://doi.org/10.1016/j.jimmuni.2020.10.022>.
 43. Uddback, I., Cartwright, E.K., Scholler, A.S., Wein, A.N., Hayward, S.L., Lobby, J., Takamura, S., Thomsen, A.R., Kohlmeier, J.E., and Christensen, J.P. (2021). Long-term maintenance of lung resident memory T cells is mediated by persistent antigen. *Mucosal Immunol.* 14, 92–99. <https://doi.org/10.1038/s41385-020-0309-3>.
 44. Parekh, V.V., Lalani, S., Kim, S., Halder, R., Azuma, M., Yagita, H., Kumar, V., Wu, L., and Kaer, L.V. (2009). PD-1/PD-L blockade prevents anergy induction and enhances the anti-tumor activities of glycolipid-activated invariant NKT cells. *J. Immunol.* 182, 2816–2826. <https://doi.org/10.4049/jimmunol.0803648>.
 45. Padte, N.N., Boente-Carrera, M., Andrews, C.D., McManus, J., Graspede, B.F., Gettie, A., Coelho-dos-Reis, J.G., Li, X., Wu, D., Bruder, J.T., et al. (2013). A glycolipid adjuvant, 7DW8-5, enhances CD8+ T cell responses induced by an adenovirus-vectored malaria vaccine in non-human primates. *PLoS One* 8, e78407. <https://doi.org/10.1371/journal.pone.0078407>.
 46. Giaccone, G., Punt, C.J.A., Ando, Y., Ruijter, R., Nishi, N., Peters, M., von Blomberg, B.M.E., Scheper, R.J., van der Vliet, H.J.J., van den Eertwegh, A.J.M., et al. (2002). A phase I study of the natural killer T-cell ligand alpha-galactosylceramide (KRN7000) in patients with solid tumors. *Clin. Cancer Res.* 8, 3702–3709.
 47. Nicol, A.J., Tazbirkova, A., and Nieda, M. (2011). Comparison of clinical and immunological effects of intravenous and intradermal administration of alpha-galactosylceramide (KRN7000)-pulsed dendritic cells. *Clin. Cancer Res.* 17, 5140–5151. <https://doi.org/10.1158/1078-0432.CCR-10-3105>.
 48. Yamasaki, K., Horiguchi, S., Kurosaki, M., Kunii, N., Nagato, K., Hanaoka, H., Shimizu, N., Ueno, N., Yamamoto, S., Taniguchi, M., et al. (2011). Induction of NKT cell-specific immune responses in cancer tissues after NKT cell-targeted adoptive immunotherapy. *Clin. Immunol.* 138, 255–265. <https://doi.org/10.1016/j.clim.2010.11.014>.
 49. Kunii, N., Horiguchi, S., Motohashi, S., Yamamoto, H., Ueno, N., Yamamoto, S., Sakurai, D., Taniguchi, M., Nakayama, T., and Okamoto, Y. (2009). Combination therapy of in vitro-expanded natural killer T cells and alpha-galactosylceramide-pulsed antigen-presenting cells in patients with recurrent head and neck carcinoma. *Cancer Sci.* 100, 1092–1098. <https://doi.org/10.1111/j.1349-7006.2009.01135.x>.
 50. Janse, C.J., Ramesar, J., and Waters, A.P. (2006). High-efficiency transfection and drug selection of genetically transformed blood stages of the rodent malaria parasite *Plasmodium berghei*. *Nat. Protoc.* 1, 346–356. <https://doi.org/10.1038/nprot.2006.53>.
 51. Hogquist, K.A., Jameson, S.C., Heath, W.R., Howard, J.L., Bevan, M.J., and Carbone, F.R. (1994). T cell receptor antagonist peptides induce positive selection. *Cell* 76, 17–27.
 52. Exley, M.A., Bigley, N.J., Cheng, O., Shaulov, A., Tahir, S.M.A., Carter, Q.L., Garcia, J., Wang, C., Patten, K., Stills, H.F., et al. (2003). Innate immune response to encephalomyocarditis virus infection mediated by CD1d. *Immunology* 110, 519–526.
 53. Anderson, R.J., Li, J., Kedzierski, L., Compton, B.J., Hayman, C.M., Osmond, T.L., Tang, C.W., Farrand, K.J., Koay, H.F., Almeida, C.F.D.S.S.E.,

- et al. (2017). Augmenting Influenza-Specific T Cell Memory Generation with a Natural Killer T Cell-Dependent Glycolipid-Peptide Vaccine. *ACS Chem. Biol.* 12, 2898–2905. <https://doi.org/10.1021/acscchembio.7b00845>.
54. Caminschi, I., Proietto, A.I., Ahmet, F., Kitsoulis, S., Shin Teh, J., Lo, J.C.Y., Rizzitelli, A., Wu, L., Vremec, D., van Dommelen, S.L.H., et al. (2008). The dendritic cell subtype-restricted C-type lectin Clec9A is a target for vaccine enhancement. *Blood* 112, 3264–3273. <https://doi.org/10.1182/blood-2008-05-155176>.
55. Almeida, C.F., Sundararaj, S., Le Nours, J., Praveena, T., Cao, B., Burugupalli, S., Smith, D.G.M., Patel, O., Brigl, M., Pellicci, D.G., et al. (2019). Distinct CD1d docking strategies exhibited by diverse Type II NKT cell receptors. *Nat. Commun.* 10, 5242. <https://doi.org/10.1038/s41467-019-12941-9>.

STAR★METHODS

KEY RESOURCES TABLE

REAGENT or RESOURCE	SOURCE	IDENTIFIER
Antibodies		
Mouse, anti-mouse CD45.1 (A20)	BioLegend, USA	Cat#110705; RRID: AB_313494
Mouse, anti-mouse CD45.2 (104)	ThermoFisher Scientific, USA	Cat#17-0454-82; RRID: AB_469400
Rat, anti-mouse CXCR6 (SA05D1)	BioLegend, USA	Cat#151106; RRID: AB_2572143
Mouse, anti-mouse CX3CR1 (SA011F11)	BioLegend, USA	Cat#149029; RRID: AB_2565938
Rat, anti-mouse monoclonal anti-CD8 α (53–6.7)	BioLegend, USA	Cat#100748; RRID: AB_2562100
Rat, anti-mouse CD19 (1D3/CD19)	BioLegend, USA	Cat#152404; RRID: AB_2629813
Armenian hamster, anti-mouse TCR β (H57-597)	BioLegend, USA	Cat#109220; RRID: AB_893624
Mouse, anti-mouse NK1.1 (PK136)	BioLegend, USA	Cat#108740; RRID: AB_2562274
Rat, anti-mouse MHC II (M5/114.15.2)	ThermoFisher Scientific, USA	Cat#56-5321-82; RRID: AB_494009
Rat, anti-mouse B220 (RA3-6B2)	BioLegend, USA	Cat#103240; RRID: AB_11203896
Armenian hamster, anti-mouse CD11c (N418)	ThermoFisher Scientific, USA	Cat#25-0114-82; RRID: AB_469590
Rat, anti-mouse CD172a (P84)	ThermoFisher Scientific, USA	Cat#17-1721-82; RRID: AB_10733158
Mouse, anti-mouse/rat XCR1 (ZET)	BioLegend, USA	Cat#148208; RRID: AB_2564364
Rat, anti-mouse CD44 (IM7)	BD Biosciences, USA	Cat#565480; RRID: AB_2739259
Armenian hamster, anti-mouse CD69 (H1.2F3)	ThermoFisher Scientific, USA	Cat#15-0691; RRID: AB_468711
Rat, anti-mouse CD62L (MEL-14)	BioLegend, USA	Cat#104418; RRID: AB_313103
Rat, anti-mouse V α 2 (B20.1)	BioLegend, USA	Cat#127825; RRID: AB_2814020
Rat, anti-mouse PD-1 (RMP1-30)	BioLegend, USA	Cat#109110; RRID: AB_572017
Rat, anti-mouse IL-12p40 (C17.8)	BioXCell	Cat#BE0051; AB_1107698
Rat IgG2a, κ isotype control (GL117)	Walter and Eliza Hall Institute Antibody facility	N/A
Rat, anti-mouse IFN- γ (R4-6A2)	BioXCell	Cat#BE0054; AB_1107692
Rat IgG1, κ isotype control (GL113)	Walter and Eliza Hall Institute Antibody facility	N/A
Mouse, anti-mouse IFNAR (MAR1-5A3)	BioXCell	Cat#BE0241; AB_2687723
Mouse IgG1, κ isotype control	BioXCell	Cat#BE0083; AB_1107784
Chemicals, peptides, and recombinant proteins		
RPL6-GLP	Lab of Prof. Gavin Painter. Holz et al. ¹²	N/A
OVA-GLP	Lab of Prof. Gavin Painter. Holz et al. ¹²	N/A
Propidium Iodide	Thermo Scientific	Cat# P3566
α -GalCer	Lab of Prof. Gavin Painter. Holz et al. ¹²	N/A
α GC-OVA-GLP	Lab of Prof. Gavin Painter. Holz et al. ¹²	N/A
β MC-OVA-GLP	This manuscript	
CpG 2006-21798	Integrated DNA Technologies, USA	Lab of Prof. Mireille Lahoud. Fernandez-Ruiz et al. ⁷
Anti-Clec9A-NVF antibody	Lab of Prof. Mireille Lahoud. Fernandez-Ruiz et al. ⁷	clone 24/04-10B4-NVF
Recombinant human interleukin-2 (IL-2)	PeproTech Inc., USA	Cat# 200-02
CellTrace Violet (CTV)	ThermoFisher Scientific, USA	Cat# C34557
SIINFEKL peptide	GenScript, China	N/A
LPS	Sigma-Aldrich, USA	Cat# L2630
Diphtheria toxin (DT)	Merck, USA	Cat# 322326
Heparin	Clifford Hallam Healthcare, Australia	Cat# 2565742
Percoll	GE Healthcare, USA	Cat# GEHE17-0891-01

(Continued on next page)

Continued

REAGENT or RESOURCE	SOURCE	IDENTIFIER
Collagenase III	Worthington Biochemical, USA	Cat# LS004183
DNase I	Sigma-Aldrich, USA	Cat# 4536282001
bisbenzimide H 33258	Sigma-Aldrich, USA	Cat# B1155
Xenolight D-luciferin potassium salt	Revvity Health Sciences Inc.	Cat# 122796
Experimental models: Organisms/strains		
<i>Plasmodium berghei</i>	The Malaria Research and Reference Reagent Resource Center; BEI resources	MRA-871
<i>Plasmodium berghei</i> - GFP/Luciferase	Janse et al. ⁵⁰	N/A
C57BL/6 mice	Animal Resources Center	Stock # 000664
OT-I mice	Hogquist et al. ⁵¹	N/A
XCR1-DTR mice	Yamazaki et al. ²⁸	N/A
CD1d ^{-/-} mice	Exley et al. ⁵²	N/A
<i>Anopheles stephensi</i>	The Malaria Research and Reference Reagent Resource Center; BEI resources	Strain: STE2/MRA-128
Software and algorithms		
Prism v10	GraphPad Software, USA	https://www.graphpad.com/
FlowJoX	Tree Star Inc.	https://www.flowjo.com/
Diva	BD Bioscience	N/A
Other		
H2-K ^b -OVA _{257–264} (SIINFEKL) tetramer	Dhilshan Jayasinghe, Gras Laboratory, La Trobe University	NA
H2-K ^b -RPL6 _{120–127} (NVFDFNNL) tetramer	Dhilshan Jayasinghe, Gras Laboratory, La Trobe University	NA
CD1d tetramer (PBS44)	Calvin Xu, Godfrey Laboratory, University of Melbourne	NA
Streptavidin-PE	ThermoFisher Scientific, USA	Cat#S866

EXPERIMENTAL MODEL AND STUDY PARTICIPANT DETAILS

Female C57BL/6 (B6), OT-I, ⁵¹ XCR1^{+/DTRvenus} ²⁸ and CD1d^{-/-} ⁵² were bred and maintained at the Department of Microbiology and Immunology, The University of Melbourne. All mice used were 6 – 12 weeks of age and littermates of the same sex were randomly assigned to experimental groups. Animals used for the generation of the sporozoites were 4 – 5-week-old male Swiss Webster mice purchased from the Monash Animal Services (Melbourne, Victoria, Australia) and housed at the School of Biosciences, The University of Melbourne, Australia. All animal experiments were in accordance with the Prevention of Cruelty to Animals Act 1986, the Prevention of Cruelty to Animals Regulations 2008, and the National Health and Medical Research Council (2013) Australian code for the care and use of animals for scientific purposes. The protocols were approved by the Melbourne Health Research Animal Ethics Committee, University of Melbourne (ethics protocols IDs: 1914923 and 20088).

METHOD DETAILS

Vaccine manufacture

All GLP vaccines were synthesized at the Ferrier Research Institute, New Zealand. Manufacture of α -GalCer-based GLP vaccines¹². Anhydrous solvents were obtained commercially. Air sensitive reactions were carried out under argon. Thin-layer chromatography (TLC) was performed on aluminum sheets coated with 60 F254 silica. Normal phase column chromatography was performed using silica gel (230–400 mesh) and the specified eluent system. Reverse phase column chromatography was performed using Biotage Isolute C18(EC) cartridges using the specified eluent system. NMR spectra were recorded on a Varian 500 MHz AR Premium Shielded Spectrometer. Chemical shifts are referenced to the residual CHD₂OD solvent peak (¹H NMR at 3.31 ppm, ¹³C NMR at 49.0 ppm). HRMS analysis was conducted on a Bruker microTOFQ mass spectrometer using electrospray ionization (ESI). Preparative HPLC purification employed a Agilent 1100 HPLC system fitted with a Phenomenex Luna C18(2), 5 μ m, 100Å, 250 \times 21.2 mm column, 40°C, 20 mL/min; Mobile phase A = 100:0.05 water/TFA; Mobile phase B = 100:0.05 MeOH/TFA, Method: 0–8 mins: 70%–100% B, 8–12 mins: 100% B, 12–13 mins: 100%–70% B, 13–15 mins: 70% B. Analytical HPLC was performed an Agilent 1260 Infinity

Quaternary HPLC equipped with an Agilent 1260 Multiple Wavelength Detector and either an Agilent 6130 single quadrupole mass spectroscopic detector using ESI (peak identification) or a Dionex Corona Ultra RS charged aerosol detector (CAD) using a Phenomenex Kinetex 100 Å C18, 2.6 µm, 3.0 × 50 mm column, 40°C, 0.5 mL/min; Mobile phase A = 100:0.05 water/TFA; Mobile phase B = 100:0.05 MeOH/TFA, Method: 0–7 mins: 30%–100% B, 7–12 mins: 100% B, 12–13 mins: 100%–30% B, 13–15 mins: 30% B. The OVA^{CD4/CD8} fusion peptide 5-azidopentanoyl-FFRKKISQAVHAAEINEAGRE SIINFEKLTEWT was prepared as previously reported.⁵³

Preparation of the β-mannosylceramide (β-ManCer, βMC)-OVA (βMC-OVA) conjugate vaccine was achieved in an analogous fashion to its α-GalCer counterpart (αGC-OVA)⁵³ (Figure S7).

Preparation of compound **2**: To a suspension of β-ManCer (**1**)³³ 50.0 mg, 58 µmol in freshly distilled dioxane (16 mL, from 2,4-DNP/H₂SO₄) was added conc. HCl (59 µL, 1.93 mmol) at room temperature under argon. The reaction was heated to 65°C (25 min) and the solvents were removed *in vacuo* to give a mixture of regioisomers with the titled compound **2** representing the major component (54.0 mg, quant.) as a white solid. This material was used directly in the next step. ¹H NMR (500 MHz, 2:1 CDCl₃:CD₃OD) δ 4.85 (1H, t, J=7.4 Hz), 4.49 (1H, s), 4.02–3.83 (5H, m), 3.73–3.68 (1H, m), 3.53 (1H, t, J=9.4 Hz), 3.44 (1H, dd, J=9.8, 2.5 Hz), 3.35 (1H, s), 3.21 (1H, ddd, J=8.8, 6.6, 2.9 Hz), 2.32 (2H, t, J=7.3 Hz), 1.81–1.70 (1H, m), 1.64–1.46 (3H, m), 1.34–1.15 (68H, s), 0.84 (6H, t, J=6.8 Hz); ¹³C NMR (126 MHz, 2:1 CDCl₃:CD₃OD) δ 174.2, 100.0, 77.1, 74.0, 73.2, 71.1, 70.4, 67.4, 67.2, 65.1, 61.6, 53.3, 34.8, 32.2, 31.7, 30.0, 30.0, 29.9, 29.7, 29.7, 29.5, 25.4, 25.2, 23.0, 14.2.

Preparation of compound **4**: To a mixture of **2** (52 mg, 58 µmol) and pNP-PAB-Cit-Val-Fmoc (**3**) (65 mg, 85 µmol) under argon was added dry pyridine (freshly distilled from CaH₂, 4 mL) followed by dry triethylamine (15 µL, 108 µmol) and the reaction stirred at room temperature (18 h). The reaction was concentrated, and the resulting residue was purified by RP C18 chromatography (water/MeOH, 40:60 to 0:100 changing to CHCl₃/MeOH, 0:100 to 60:40) to afford the titled compound **4** (50 mg, 58% from **1**) as an off white solid. ¹H NMR (500 MHz, 2:1 CDCl₃:CD₃OD) δ 9.56 (1H, s), 7.90 (1H, d, J=7.7 Hz), 7.73 (2H, d, J=7.5 Hz), 7.58 (2H, d, J=7.5 Hz), 7.52 (2H, d, J=8.2 Hz), 7.38–7.32 (2H, m), 7.27 (4H, ddd, J=7.5, 5.7, 1.6 Hz), 6.51 (1H, d, J=8.2 Hz), 5.06 (1H, t, J=12.9 Hz), 5.00–4.89 (2H, m), 4.51 (1H, q, J=7.6, 7.2 Hz), 4.45–4.37 (1H, m), 4.30 (1H, dd, J=10.9, 6.6 Hz), 4.19 (1H, t, J=6.9 Hz), 4.11–4.04 (1H, m), 3.99–3.92 (1H, m), 3.89–3.78 (2H, m), 3.78–3.71 (2H, m), 3.68 (1H, dd, J=12.0, 5.5 Hz), 3.65–3.59 (1H, m), 3.55 (1H, t, J=9.6 Hz), 3.41 (1H, ddd, J=14.6, 9.3, 3.3 Hz), 3.17 (2H, dddd, J=12.5, 8.2, 6.1, 3.2 Hz), 3.06 (1H, dt, J=13.3, 6.4 Hz), 2.38–2.21 (2H, m), 2.05 (1H, h, J=6.7 Hz), 1.86 (1H, dt, J=13.8, 6.9 Hz), 1.72–1.43 (7H, m), 1.34–1.15 (70H, s), 0.91 (6H, dd, J=9.1, 6.7 Hz), 0.84 (6H, t, J=6.7 Hz); ¹³C NMR (126 MHz, 2:1 CDCl₃:CD₃OD) δ 174.9, 173.1, 170.9, 161.0, 157.5, 156.9, 144.2, 144.0, 141.6, 138.2, 132.8, 129.9, 129.1, 128.1, 127.4, 125.4, 125.3, 120.4, 120.3, 100.0, 76.8, 75.0, 74.0, 71.7, 71.0, 68.2, 67.5, 67.3, 66.8, 61.9, 61.1, 53.6, 52.1, 47.5, 39.4, 34.9, 32.2, 31.3, 30.02, 29.99, 29.89, 29.86, 29.8, 29.68, 29.66, 29.5, 28.9, 26.7, 25.7, 25.4, 23.0, 19.4, 18.2, 14.2; HRMS (ESI-pos): calcd for C₈₄H₁₃₆O₁₆N₆Na [M+Na]⁺ m/z 1507.9905 found m/z 1507.9894.

Preparation of compound **5**: To a solution of **4** (22 mg, 15 µmol) in dry DMF (1 mL) at 0°C under argon was added piperidine (90 µL, 0.72 mmol) and the reaction was allowed to warm to room temperature (30 min). The reaction was concentrated, and the resulting residue was purified by RP C18 chromatography (water/MeOH, 40:60 to 0:100 changing to CHCl₃/MeOH, 0:100 to 60:40) to afford the titled compound **5** (13 mg, 70%) as an off white solid. ¹H NMR (500 MHz, 2:1 CDCl₃:CD₃OD) δ 7.50 (2H, d, J=8.2 Hz), 7.26 (2H, d, J=8.1 Hz), 5.09 (1H, d, J=12.3 Hz), 4.96–4.87 (2H, m), 4.53 (1H, dd, J=9.4, 4.6 Hz), 4.36 (1H, s), 4.07–4.02 (1H, m), 3.84–3.76 (2H, m), 3.76–3.59 (5H, m), 3.54 (1H, t, J=9.5 Hz), 3.38 (1H, dd, J=9.4, 3.3 Hz), 3.15–3.09 (3H, m), 2.28 (2H, dp, J=14.9, 7.4 Hz), 2.13 (1H, h, J=6.8 Hz), 1.85 (1H, dq, J=13.1, 7.2 Hz), 1.73 (1H, dq, J=14.4, 7.4 Hz), 1.68–1.50 (6H, m), 1.34–1.15 (68H, m), 1.00 (6H, dd, J=6.9, 3.0 Hz), 0.83 (6H, t, J=6.9 Hz); ¹³C NMR (126 MHz, 2:1 CDCl₃:CD₃OD) δ 174.9, 170.7, 168.7, 161.1, 156.9, 138.2, 132.8, 129.1, 120.3, 100.0, 76.8, 75.0, 74.0, 71.8, 70.9, 68.2, 67.4, 66.7, 61.8, 58.9, 53.9, 52.1, 39.1, 35.0, 32.2, 30.6, 30.01, 29.99, 29.97, 29.94, 29.91, 29.90, 29.87, 29.85, 29.8, 29.7, 29.64, 29.63, 29.5, 29.4, 28.9, 26.5, 25.7, 25.4, 23.0, 18.5, 17.7, 14.2; HRMS (ESI-pos): calcd for C₆₉H₁₂₇O₁₄N₆ [M + H]⁺ m/z 1263.9405 found m/z 1263.9383.

Preparation of Compound **7**: To a solution of **5** (32 mg, 25 µmol) and exo-BCN-pNP (**6**) (13 mg, 40 µmol) in dry DMF (1 mL) under argon was added dry triethylamine (16 µL, 115 µmol). The reaction was stirred at room temperature (18 h) then diluted with CH₂Cl₂ (5 mL) and concentrated *in vacuo*. The resulting residue was purified by RP C18 chromatography (water/MeOH, 20:80 to 0:100 changing to CHCl₃/MeOH, 0:100 to 80:20) to afford the titled compound **7** (26 mg, 71%) as a white solid. ¹H NMR (500 MHz, 2:1 CDCl₃:CD₃OD) δ 9.54 (1H, s), 7.84 (1H, d, J=7.9 Hz), 7.51 (2H, d, J=8.1 Hz), 7.27 (2H, d, J=8.1 Hz), 6.46 (1H, d, J=7.6 Hz), 6.20 (1H, d, J=8.5 Hz), 5.07 (1H, d, J=12.3 Hz), 4.97–4.89 (2H, m), 4.50 (1H, q, J=6.8 Hz), 4.37 (1H, s), 4.06 (1H, d, J=10.1 Hz), 3.95 (2H, t, J=7.3 Hz), 3.90 (1H, dd, J=10.9, 7.0 Hz), 3.84–3.78 (2H, m), 3.76–3.72 (2H, m), 3.67 (1H, dd, J=12.1, 5.5 Hz), 3.64–3.57 (1H, m), 3.53 (1H, t, J=9.5 Hz), 3.38 (1H, dd, J=9.5, 3.3 Hz), 3.16 (2H, dq, J=12.5, 7.5 Hz), 3.06 (1H, dt, J=13.3, 6.4 Hz), 2.36–2.20 (6H, m), 2.13–1.91 (3H, m), 1.92–1.78 (1H, m), 1.71–1.42 (7H, m), 1.34–1.15 (72H, m), 0.91 (6H, dd, 6.7 Hz), 0.83 (6H, t, J=6.8 Hz), 0.73–0.59 (3H, m); ¹³C NMR (126 MHz, 2:1 CDCl₃:CD₃OD) δ 174.9, 170.9, 161.0, 157.9, 156.9, 138.2, 132.8, 129.1, 120.4, 100.0, 99.1, 76.8, 75.0, 74.0, 71.7, 70.9, 70.0, 68.2, 67.5, 66.8, 61.9, 60.9, 53.6, 52.1, 39.4, 34.9, 33.5, 32.2, 31.3, 30.02, 29.98, 29.95, 29.92, 29.88, 29.85, 29.8, 29.68, 29.65, 29.64, 29.5, 28.9, 26.7, 25.7, 25.4, 23.9, 23.3, 23.0, 21.5, 19.4, 18.0, 14.2; HRMS (ESI-pos): calcd for C₈₀H₁₃₈O₁₆N₆Na [M+Na]⁺ m/z 1462.0062 found m/z 1462.0033.

Preparation of compound **9**: A mixture of **7** (1.1 mg, 0.8 µmol) and peptide 5-azido-pentanoyl-FFRKKISQAVHAAEINEAGRESIINFEKLTEWT (**8**) (3.2 mg, 0.8 µmol) in DMSO (200 µL, HPLC grade) under argon was stirred at ambient temperature (18 h). The material was purified using preparative HPLC and the combined fractions were lyophilized to afford **βMC-OVA GLP (9)** (2.81 mg, 64%, 98% pure by HPLC-CAD) as a white solid. HRMS (ESI-pos): calcd for C₂₆₉H₄₃₂O₇₀N₆₁ [M+3H]³⁺ m/z

1879.0701 found m/z 1879.0727; calcd for $C_{269}H_{433}O_{70}N_{61}$ [M+4H] $^{4+}$ m/z 1409.5544 found m/z 1409.5601; calcd for $C_{269}H_{434}O_{70}N_{61}$ [M+5H] $^{5+}$ m/z 1127.8450 found m/z 1127.8468; calcd for $C_{269}H_{435}O_{70}N_{61}$ [M+6H] $^{6+}$ m/z 940.0387 found m/z 940.0439.

T cell transfer

Naive OT-I CD8 $^{+}$ T cells were isolated by negative selection from the spleen as previously described.⁷ Briefly, tissues were disrupted by passing through 70 μ m cell strainers and red cells lysed. Single cell suspensions were labeled with a cocktail of rat monoclonal antibodies specific for CD4, MHC Class II, macrophages and neutrophils prior to incubating with BioMag goat anti-rat IgG beads (QIAGEN, Chadstone, VIC, Australia) and separating using a magnet. Enriched naive CD8 $^{+}$ T cells were counted, and their purity analyzed by staining with anti-CD8 α (BioLegend, USA) and anti-V α 2 TCR (BioLegend, USA) antibodies. Cell counts were adjusted to 2.5×10^5 transgenic T cells/mL in PBS and mice were injected with 200 μ L i.v. In some experiments where *in vivo* OT-I cell proliferation was assessed, the enriched CD8 $^{+}$ T cells were adjusted to 10×10^6 cells/mL in PBS/0.1% BSA. The sample was then labelled with 0.5 μ L of CellTrace Violet (CTV, ThermoFisher, USA, final concentration 5 mM) for 10 min in the dark at 37°C. Cells were washed three times with RPMI/2% FCS (RP-2) and adjusted to the indicated concentration in 200 μ L PBS for i.v. injection.

Vaccination

GLP vaccines (Figure S1) were formulated into a tween, histidine sucrose solubilisation matrix⁴⁶ through reconstitution with PBS. Mice were vaccinated i.v. with 0.135 nmol of GLP (in 200 μ L of PBS) or were injected with naive OT-I cells one day prior to vaccination with an OVA expressing GLP vaccine. Mice were prime boosted 9 – 60 days post-priming with either 0.135 nmol of GLP vaccine or 8 μ g of an anti-Clec9A antibody (clone 24/04-10B4-NVF) genetically fused to NVFDFNNL and 5 nmol of CpG 2006–21798 (Integrated DNA Technologies, USA).^{7,54}

In vitro OT-I cell activation

Spleens isolated from OT-I and naive B6 mice were meshed through 70 μ m cell strainers. B6 splenocytes were washed with sterile RPMI/10% FCS (RP-10) and resuspended in 5 mL of RP-10. 0.5 μ g/mL of SIINFEKL peptide (Genscript, China) was added to the cell suspension and incubated in a 37°C water bath for 1 h, with gentle shaking every 15 min. Peptide-pulsed B6 cells were then washed three times with RP-10 to remove unbound peptide. Peptide-pulsed B6 splenocytes and OT-I cells were co-cultured in T175 flasks containing 5 μ g of LPS (Sigma Aldrich, USA) and 10 U/mL of recombinant human IL-2 (PeproTech Inc., USA) for 4 days at 37°C and 5% CO₂ in a humidified incubator. Cells were split 1:1 on both days 2 and 3 with RP-10 (no additional IL-2 or LPS). At day 4 post-culture, cells were harvested and washed three times with RP-10. The purity and cell count of *in vitro*-activated OT-I cells was calculated and mice were injected with 5×10^6 OT-I cells. The following day these mice were treated with 0.135nmol of GLP vaccine or 0.135nmol of α -GalCer.

In vivo cDC1 depletion

To deplete XCR1 $^{+}$ cDC1, B6 or XCR1-DTRvenus mice were treated i.p. with 25 ng/g body weight of diphtheria toxin (DT, Merck, USA) diluted in 200 μ L PBS every two days, starting from day –1 to day 3 post-vaccination (Figures 3 and S3A–S3C), days –1 and 1 post-vaccination (Figure S4A), day 7 only (Figures S3D and S3E), or day 20 only (Figure 5F).

Organ harvest and processing

Blood was collected by cardiac puncture into Eppendorf tubes containing 10 μ L of heparin (200 U/ml, Clifford Hallam Healthcare, Australia). Red cells were lysed by adding 500 μ L of lysis buffer and incubating for 5 min before centrifuging at 1,600 rpm 5 min 4°C. Pellets were lysed an additional two times before being resuspended in 200 μ L of FACS buffer. The entire sample was used for FACS analysis. Spleens and/or peripheral lymph nodes (LNs) were harvested into cold RP-2, meshed through a 70 μ m cell strainer, and then washed with 10 mL of RP-2. To lyse red blood cells, the resulting cell pellets were resuspended with ~1 mL of lysis buffer for ~1 min before washing with 10 mL of RP-2. Cells were resuspended in 10 mL of FACS buffer and 1/20th of the spleen, or the whole LN, was used for tetramer and/or antibody staining. Livers were harvested in 10 mL of cold RP-2 containing 50 μ L of heparin (200 U/ml, Clifford Hallam Healthcare, Australia). Single-cell suspensions were produced by grinding the organs through a 70 μ m cell strainer and then washing with 50 mL of RPMI. To purify liver lymphocytes, the cell pellets were resuspended in 30 mL of 35% Percoll (GE Healthcare, USA), inverted 3–5 times to ensure thorough mixing, and centrifuged at 500 g for 20 min at room temperature, no brake. Red cells were removed from the pellet by adding 5 mL of lysis buffer, incubating for 5min, then washing with 50mL of RP-2. WBC pellets were resuspended in 2 mL of FACS buffer and 1/4th of the liver lymphocyte population was used for flow cytometry analysis. For experiments aimed to assess DC populations, livers and spleens were finely chopped by scissors into small pieces in 1 mg/mL of collagenase III (Worthington Biochemical, USA) and 20 μ g/mL of DNase I (Sigma Aldrich, USA) and then incubated at 37°C for 30 min. Both organ samples were then processed accordingly, as described above.

FACS staining and analysis

Lymphocytes were stained with RPL6 (H-2K b -RPL6_{120–127}) or OVA (H-2K b -OVA_{257–264})-specific tetramers for 1 h at room temperature before staining with monoclonal antibodies for: CD44 (IM7) from BD Biosciences (USA), NK1.1 (PK136), XCR1 (ZET), CD8 α (53–6.7), CD45.1 (A20), B220 (RA3-6B2), TCR β (H57-597), CXCR6 (SA051D1), CX3CR1 (SA011F11), CD19 (1D3/CD19), PD-1 (RMP1-30),

CD62L (MEL-14), V α 2 (B20.1) from Biolegend (USA), and CD69 (H1.2F3), CD45.2 (104), MHC II (M5/114.15.2), CD11c (N418), and CD172a (P84) from ThermoFisher Scientific (USA). In some experiments, cells were treated with Fc Block (2.4G2) for 10 min prior to staining with an α -GalCer analogue (PBS-44 – a gift from Prof. Paul Savage, Brigham-Young University, UT, USA)-loaded CD1d tetramer produced in-house⁵⁵ at 4°C for 30 min. Dead cells were excluded by Propidium Iodide (ThermoFisher Scientific, USA) staining. Single-color positive control samples were used to adjust compensation and cells were analyzed by flow cytometry on an LSR Fortessa (BD Biosciences, USA), or Cytek Aurora using FlowJo software (Tree Star Inc., USA). Gating strategies for analyzing single live cells, NKT cells, dendritic cells, tetramer $^+$ CD8 $^+$ T cells and OT-I cells are outlined in [Figure S2](#).

Malaria challenge

Plasmodium berghei ANKA (PbA) parasite maintenance was performed as previously described.¹⁶ Briefly, infections of naive Swiss mice were carried out by i.p. inoculation of PbA infected RBCs obtained from a donor mouse between the first and fourth passages from a cryopreserved stock. Parasitemia was monitored by Giemsa smear and exflagellation quantified 3 days post infection. 1 μ L of tail prick blood was mixed with 100 μ L of exflagellation media (RPMI [Invitrogen] supplemented with 10% v/v fetal bovine serum, pH 8.4), incubated for 15 min at 20 °C, and exflagellation events per 1x10⁴ red blood cells were counted. *A. stephensi* mosquitoes were allowed to feed on anesthetized mice once the exflagellation rate was assessed between 12 and 15 exflagellation events per 1x10⁴ red blood cells. 22 days after biting, salivary glands were dissected and checked for the presence of sporozoites. B6 mice were infected intravenously with 200 or 3,000 freshly isolated PbA sporozoites diluted in 200 μ L PBS, or 30,000 PbA-luciferase sporozoites diluted in 200 μ L PBS.⁵⁰ To assess blood-stage parasitemia, 2 μ L of tail blood was diluted in 50 μ L of PBS and stained with 5 pg/mL bisbenzimidole H 33258 (Sigma Aldrich, USA) in 50 μ L of PBS for 1 h at 37°C and 5% CO₂ in a humidified incubator. Samples were then diluted with 100 μ L PBS before being analyzed by flow cytometry. Parasitemia after challenge with 200 sporozoites was measured on day 6, 7, 8, 10 and day 12 post-infection, with mice lacking parasitemia by day 12 classified as having sterile immunity. In cases where mice were challenged with 3,000 sporozoites, blood-stage parasitemia was measured on day 5–8, 10 and 12. For 3,000 sporozoite challenges, naive groups are not shown but were similar in number to the naive 200 sporozoite challenge groups and all mice became parasitic, indicating infection.

IVIS imaging

B6 mice were challenged i.v. with 30,000 luciferase-expressing sporozoites and parasite burden assessed at 42 h using whole body imaging (IVIS, Xenogen, USA). Mice were anesthetized in an oxygen-rich induction chamber with 3.5% isoflurane and shaved. Whole body imaging was performed 10 min after i.p. injection with 0.05 mg/g body weight Xenolight D-luciferin potassium salt (Revvity Health Sciences Inc.). Bioluminescence imaging was acquired with 21.7 cm field of view for whole body imaging, with a medium binning factor, and exposure time of 5 min. For bioluminescence quantification, regions of interest (ROIs) were drawn using the software Living Image 3.0 and average radiance (p/s/cm²/sr) was determined.

QUANTIFICATION AND STATISTICAL ANALYSIS

Figures were generated using GraphPad Prism 10. Data are shown as mean \pm SEM or mean \pm SD, as indicated in the figure legends. Data was log transformed, then a one-way ANOVA with Tukey's multiple comparison test, one-way ANOVA with Dunnett's multiple comparison test, one-way ANOVA with Sidak multiple comparison test, Mann-Whitney U-test or students t-test was performed. To compare survival after challenge, groups were compared using Fisher's exact test. To estimate the half-life of liver Trm cells, cell counts were log2-transformed and analyzed by simple linear regression on GraphPad Prism. The statistical tests performed on the data are indicated in the figure legends and results, along with sample size (n) indicating the number of animals used and the number of replicate experiments. P-values <0.05 (*), <0.01 (**), 0.001 (***) or 0.0001 (****) were considered statistically significant.